A framework for assessing harvest strategy choice when considering multiple interacting fisheries and a changing environment: The example of eastern Bering Sea crab stocks

André E. Punt[1], Michael G. Dalton[2], Benjamin Daly[3], Tyler Jackson[3], W. Christopher Long[3], William T. Stockhausen[2], Cody Szuwalski[2], and Jie Zheng[4]

[1]School of Aquatic and Fishery Sciences, Box 355020, University of Washington, Seattle, WA 98195
[2]Alaska Fisheries Science Center, National Marine Fisheries Service, NOAA, 7600 Sand Way Point Way, NE, Seattle WA 98115
[3]Alaska Fisheries Science Center, National Marine Fisheries Service, NOAA, 301 Research Court Kodiak , AK 99615
[4]Alaska Department of Fish and Game, 351 Research Ct, Kodiak, AK 99615

Abstract

Ecosystem Based Fisheries Management aims to broaden the set of factors included in assessments and management decision making but progress with implementation remains limited. We developed a framework that examines the consequences of temporal changes in temperature and ocean pH on yield and profit of multiple interacting stocks including eastern Bering Sea (EBS) snow, southern Tanner, and red king crab. Our analyses integrate experimental work on the effects of temperature and ocean pH on growth and survival of larval and juvenile crab and monitoring data from surveys, fishery landings, and at-sea observer programs. The impacts of future changes in temperature and ocean pH on early life history have effects that differ markedly among stocks, being most pessimistic for Bristol Bay red king crab and most optimistic for EBS snow crab. Our results highlight that harvest control rules that aim to maximize yield lead to lower profits than those that aim to maximize profit. Similarly, harvest control rules that aim to maximize profit lead to lower yields than those that aim to maximize yield, but differences are less pronounced. Maximizing profits has conservation benefits, especially when the implemented harvest control rule reduces fishing mortality if population biomass is below a threshold level.

Keywords: Bycatch, control rules MSY, MEY, North Pacific, ocean acidification, red king crab, snow crab, southern Tanner crab

Corresponding author: A.E. Punt
a. *Email*: aepunt@uw.edu
b. *Phone*: 1-206-221-6319
c. *Fax* : 1-206-685-7471

1. Introduction

NOAA's Ecosystem Based Fisheries Management (EBFM) Policy defines EBFM as "*a systematic approach to fisheries management in a geographically specified area that contributes to the resilience and sustainability of the ecosystem; recognizes the physical, biological, economic, and social interactions among the affected fishery related components of the ecosystem, including humans; and seeks to optimize benefits among a diverse set of societal goals*" (NMFS, 2016). Implementation of EBFM has, however, lagged behind broad policy statements (e.g., Pitcher, et al., 2008; Skern-Mauritzen et al., 2016) although aspects of EBFM are included in management processes for several fisheries and in several regions (Marshall et al., 2018; NPFMC, 2019; Townsend et al., 2019). These include adding environmental factors into stock assessments (e.g., Schirripa et al., 2009; Skern-Mauritzen et al., 2016), identification and protection of essential fish habitat (e.g. Laman et al., 2017), mitigation of fisheries impacts on protected, endangered and threatened species (e.g., Wade, 1998), the development of management strategy evaluation frameworks that account for ecosystem effects and include performance metrics that reflect ecosystem considerations (e.g. Fulton et al., 2019), and development of approaches for including climate change in forecasts (Hollowed et al., 2020).

Bering Sea crab populations support valuable commercial fisheries (e.g., Garber-Yonts and Lee, 2021), which are currently managed using harvest control rules and biologically-based reference points (NPFMC, 2008; ADF&G, 1990). However, the stock assessments used to estimate management reference points do not explicitly include environmental factors or projections that reflect a changing climate. Three of the four major crab stocks in the Bering Sea are eastern Bering Sea snow crab (*Chionoecetes opilio*), southern Tanner crab (*Chionoecetes bairdi*) in the eastern Bering Sea and red king crab (*Paralithodes camtschaticus*) in Bristol Bay (Fig. 1). There are targeted fisheries for each of these stocks ("directed fisheries"), but there can be considerable bycatch of the other stocks owing to overlapping distributions[1,2]. Consequently, changes to the total allowable catches for one stock can impact the available biomass of other species.

Understanding how climate change will affect these stocks is critical for stock management. Ocean acidification alters embryonic development in red king crab and southern Tanner crab

[1] It is possible to land some of incidental catch of "non-target" crab species (Daly, ADF&G, pers commn), but the amount landed is sufficiently small not to warrant inclusion in the base version of the model.

[2] The fourth major stock is golden king crab (*Lithodes aequispinus*) in the Aleutian Islands but the directed fishery for this stock does not interact with those for EBS snow crab, EBS southern Tanner crab, and Bristol Bay red king crab.

(Long et al., 2013a; Swiney et al., 2016) but not in snow crab (Long, unpublished data). For example, ocean acidification reduces southern Tanner crab larval hatching success by more than 70% (Swiney et al., 2016), has a negative effect on survival of larvae of both species, and has significant negative carryover effects on the survival of larvae from exposure during embryonic development (Long et al., 2013a, 2016). Juvenile red king crab and southern Tanner crab suffer decreased growth and increased mortality in low pH waters (Long et al., 2013b). Further, ocean acidification has sub-lethal effects on crab that are likely to affect their fitness including increased respiration (Long et al., 2019), increased hemocyte mortality (Meseck et al., 2016), internal and external dissolution of the exoskeleton (Dickenson et al., 2021), alteration of exoskeleton mechanical properties (Coffey et al., 2017), and altered gene expression patterns (Stillman et al., 2020). Temperature has a major effect on crab growth and survival, with growth generally increasing with temperature until temperatures become high enough to become stressful, at which point growth decreases and mortality increases (Long and Daly, 2017; Stoner et al., 2010; Yamamoto et al., 2015; Siikavuopio et al., 2017). In part because of species-specific thermal tolerances, temperature also has a major influence on crab distribution in the Bering Sea (Loher and Armstrong, 2005; Chilton et. al., 2010; Szuwalski et al., 2021; Murphy, 2020; Fedewa et al., 2020). Relatively little work has been done examining the combined effects of temperature increases and OA on these crab species, but there is a synergistic increase in mortality when the two stressors are combined in juvenile red king crab (Swiney et al., 2017).

Management advice for crab stocks in the Bering Sea and Aleutian Islands is based on the application of harvest control rules. The results of the stock assessments for these stocks are used to apply Overfishing Limit (OFL) control rules. The OFL control rules aim to manage stocks to achieve maximum sustainable yield and are formed into a tier system, where the OFLs for stocks in higher (i.e., more data rich) tiers are based on estimates of F_{MSY} (the fishing mortality rate corresponding to MSY) and those in lower tiers are based on proxies for F_{MSY} (NFMFC, 2008). EBS snow crab, EBS southern Tanner crab and Bristol Bay red king crab are in tier 3 where the proxy for F_{MSY} is $F_{35\%}$ (the fishing mortality rate that reduces spawning biomass-per-recruit to 35% of its unfished level). The acceptable biological catch (ABC; the OFL reduced by a ‘buffer’ to account for scientific uncertainty) is the upper limit for the total allowable catch, which is set by the State of Alaska.

The harvest control rules are meant to scale fishery removals proportionately to stock status, yet the explicit inclusion of environmental uncertainties into the management process is an ongoing challenge. Environmental variables are well documented (e.g., Siddon, 2020) but the quantitative incorporation of varying environmental factors continues to be in development for Bering Sea crab stocks. Some harvest control rules have been revised in recent years to take a more precautionary approach in light of recent environmental changes in the Bering Sea (e.g., Heller-Shipley et al., 2021), and efforts are underway to develop alternative management tools for addressing effects of climate change on Alaska marine resources such as stock-specific risk tables (Dorn and Zador, 2020) and ecosystem and socioeconomic profiles (e.g., Shotwell et al., 2019).

This paper constructs a framework that considers multiple stocks that interact through technical (i.e., bycatch) interactions and whose recruitment is driven by both reproductive output through a stock-recruitment relationship and climate-driven environmental variables related to sea surface temperature, bottom temperature and ocean pH. Other environmental variables may impact population-dynamic processes for Bering Sea crabs but we restricted this paper to those variables for which there is experimental work to quantify effects. The framework is applied to the fisheries for EBS snow and southern Tanner crab and Bristol Bay red king crab. Resulting changes in bioeconomic reference points (MSY and maximum economic yield, MEY), and performances of alternative harvest control rules are evaluated for each stock. Here we extend the analyses of Punt et al. (2020) who estimated maximum economic yield for EBS southern Tanner crab and Bristol Bay red king crab given the effects of ocean acidification by including snow crab (i.e., the stock that constitutes the largest landings of any EBS crab stock), by including temperature effects on growth and survival, and by including capital costs in the economic model.

2. Methods

2.1 Overview

The three stocks of Bering Sea crabs are modelled using two models: (a) a post-recruitment model with an annual time-step that represents the crab that are monitored during research surveys and subject to fishery-related mortality, and (b) a pre-recruitment model with a 6-day time-step that considers the larval and juvenile stages and computes the probability of survival from hatching to reaching the first size included in the post-recruitment model, as well as the time from hatching until recruitment to the post-recruitment model (Fig. 2). The pre- and post-recruitment models are size-structured. Three “fleets” (the directed fishery for EBS snow crab, the directed fishery for EBS southern Tanner crab, and the directed fishery for Bristol Bay red king crab) are included in the post-recruitment model. The baseline case for the model is that only catches of the target species are assumed to be landed (e.g., catches of southern Tanner crab in the directed snow crab fishery are assumed to be discarded). The alternative case, that crab that would be retained by a directed fishery are landed irrespective of which fishery they are caught in is examined for the purpose of examining sensitivity when estimating MEY. The post-recruitment model is fitted to data on survey estimates of biomass and the associated size-composition information, on landings and discards by the directed fishery (in weight), and on the size-composition of the landings and the total catch. The pre-recruitment model is parameterized using the results of experiments that relate survival and growth of larvae and juveniles to changes in temperature and pH.

The fitted post-recruitment model forms the basis for the calculation of reference points under the assumption of deterministic dynamics (i.e., ignoring future variation about the stock-recruitment relationship), as is standard practice, and forms the basis for deterministic and stochastic projections.

2.2 Post-recruitment population dynamics model

The post-recruitment dynamics of the stocks are modelled using a population dynamics model that is a simplification of the stock assessment models applied to crab stocks in the Bering Sea and Aleutian Islands (BSAI) region of Alaska (e.g., Zheng and Siddeek, 2020; Szuwalski, 2020; Stockhausen, 2020) in which only males are modelled, fewer size-classes are used, and no consideration is taken of shell condition. These simplifications were made for computational reasons, but will not impact the results markedly as the fisheries are only allowed to retain males. Mature male biomass (MMB) at the time of mating (taken to be 15 February) is used as a proxy for fertilized egg production in these models, consistent with how management advice is provided for BSAI crab (NPFMC, 2008). The basic dynamics of each population are[3]:

$$\underline{N}_{y+1} = \mathbf{X}\mathbf{S}_y \underline{N}_y + \underline{R}_{y+1} \tag{1}$$

where $\underline{N}_y$ is the vector of numbers-at-size (males only) at the start of year y, $\mathbf{X}$ is the growth transition matrix (assumed to be lower triangular; Supplementary Appendix A), $\mathbf{S}_y$ is the survival matrix for year y, and $\underline{R}_y$ is the vector of recruits for year y. The matrix $\mathbf{S}_y$ is diagonal with elements:

$$S_{y,i,i} = e^{-(M+F_{y,i})} \tag{2}$$

[3] For ease of presentation the equations in this section do not include a superscript for species, except where necessary to define technical interactions.

where M is the instantaneous rate of natural mortality (assumed to be time-invariant), $F_{y,i}$ is the fishing mortality during year y for animals in length-class i:

$$F_{y,i} = \sum_f \tilde{F}_y^f V_i^f (R_i^f + \Omega(1 - R_i^f)) \tag{3}$$

$\tilde{F}_y^f$ is the fully-selected fishing mortality by fleet f (the directed fisheries for snow crab, southern Tanner crab and Bristol Bay red king crab) during year y, V_i^f is the selectivity for animals in size-class i by fleet f, R_i^f is the probability of retention by fleet f for animals in size-class i, and Ω is the discard mortality rate (0.2 for Bristol Bay red king crab; 0.3 for snow crab and 0.321 for southern Tanner crab; Zheng and Siddeek, 2020; Szuwalski, 2020; Stockhausen, 2020). Selectivity here reflects the combined effects of gear selectivity as well as the spatial distribution of crab of different sizes. Selectivity is specified to have a maximum of one.

Fully-selected fishing mortality is modelled using a separable model. For fleet f, the fishing mortality for a species s, during year y is given by:

$$\tilde{F}_y^{f,s} = F^{\mathrm{ref},f} \gamma^{f,s} e^{\eta_y^f} \tag{4}$$

where $F^{\mathrm{ref},f}$ is the reference level of fully-selected fishing mortality for fleet f, $\gamma^{f,s}$ is the ratio of the fully-selected fishing mortality for stock s relative to a reference stock for fleet f (the reference stock is arbitrarily set to snow crab for the directed snow crab fleet, southern Tanner crab for the directed southern Tanner fleet and red king crab for red king crab fleet), and η_y^f is the annual deviation in fully-selected fishing mortality for fleet f during year y. Equation 4 implies that the trend in fully-selected fishing mortality among stocks is the same given a fleet and reduces the number of estimable parameters markedly.

Under the assumption that the fishery occurs instantaneously in the middle of the model year (which starts on 1 July) after half of natural mortality, the retained catches (in weight) and total catches (in weight) during year y, $\tilde{C}_y^{\mathrm{R}}$ and $\tilde{C}_y^{\mathrm{T}}$, are:

$$\tilde{C}_y^{\mathrm{R},f} = \sum_i w_i R_i^f V_i^f \tilde{F}_y^f N_{y,i} e^{-0.5M} (1 - e^{-F_{y,i}}) = \sum_i w_i C_{y,i}^{\mathrm{R},f} \tag{5a}$$

$$\tilde{C}_y^{\mathrm{T},f} = \sum_i w_i V_i^f \tilde{F}_y^f N_{y,i} e^{-0.5M} (1 - e^{-F_{y,i}}) = \sum_i \tilde{C}_{y,i}^{\mathrm{T},f} = \sum_i w_i C_{y,i}^{\mathrm{T},f} \tag{5b}$$

where w_i is the average weight of a male crab in length-class i, and $C^{\mathrm{R},f}_{y,i}$ and $C^{\mathrm{T},f}_{y,i}$ are respectively the retained and total catches by fleet f of animals in size-class i during year y in numbers.

Under the assumption that the fishery occurs before mating, and that mating occurs on 15 February of year y+1, the mature male biomass for year y, MMB_y, is computed using the equation:

$$MMB_y = \sum_i N_{y,i}\, m_i\, e^{-0.625 M_y} e^{-F_{y,i}} \qquad (6)$$

where m_i is the fecundity of a crab in size-class i, and 0.625 is the proportion of the year between 1 July and 15 February. Density-dependence is assumed to impact the survival rate of animals that reach the first juvenile stage (i.e., survival for the first juvenile stage is assumed to be density-independent; Sainte-Marie and Lafrance, 2002; Daly et al., 2009), and is modelled based on the mature male biomass at the time of mating for consistency with how management advice is provided, and projections conducted, for crab stocks in Bering Sea (NPFMC, 2008).

Following Punt et al. (2014a), the number of animals entering the first stage of the model is governed by a Ricker stock-recruitment relationship and accounts for the fact that multiple year-classes contribute to recruitment to the first size-class in the post-recruitment model[4]:

$$R_y = R_0 \sum_{L=1}^{10} \Omega_{y-L} P_{y-L,y} \Delta_{y-L} \frac{MMB_{y-L}}{MMB_0} e^{1.25\ell n(5h)(1-\Delta_{y-L} MMB_{y-L}/MMB_0)} e^{\varepsilon_{y-L}-\sigma_R^2/2} \qquad (7)$$

where MMB_y can be a historical or projected value, L is a potential lag between hatching and recruitment to the first size-class in the post-recruitment model, Ω_y is survival rate from the juvenile stage to recruiting to the first size-class in the post-recruitment model for animals spawned during year y (scaled to that for an unfished state), $P_{y\text{-}L,y}$ is the proportion of the eggs that were hatched during year y-L that recruited during year y given they survived, and recruited during year y, Δ_y is the survival rate from hatching to the first juvenile stage for animals spawned during year y (scaled to that for an unfished state), $\varepsilon_y \sim N(0;\sigma_R^2)$, and σ_R is the standard deviation of the log-deviations about Equation 7. R_0 and MMB_0 are respectively the recruitment and MMB in an unfished state and h is the 'steepness' of Equation 7 (the expected

[4] Punt et al. (2014a, 2016) examined sensitivity to the form of the stock-recruitment relationship and found it be inconsequential given that F_{MSY} is forced to occur at $F_{35\%}$ in the absence of ocean acidification effects.

numbers entering the first stage of the model when MMB=0.2MMB_0, expressed as a proportion of R_0; Francis [1992]).

The parameters of the model that are estimated by fitting it to the data collected from the fishery and during surveys for each species (Supplementary Table A.1) are: (a) the parameters that define the growth transition matrix, (b) selectivity-at-size for each fleet and area for which there are catches, (c) selectivity-at-size for crab in the surveys conducted by the US National Marine Fisheries Service (NMFS), (d) the probability of being landed and retained given being caught in the directed pot fishery by area, (e) the initial (1997) size-structure of the population, (f) the fully-selected fishing mortality rates for each fleet and year when the directed catch was non-zero, (g) the parameters that relate fully-selected fishing mortality for the target species to those for the non-target species (the γ parameters), (h) the mean recruitment, $\overline{R}$ and (i) the deviations in the recruitment about mean recruitment, ε_y, i.e. $R_y = \overline{R}e^{\varepsilon_y}$.

Given the small number of size-classes, many of the estimates of selectivity and retention were either equal to 0 or to 1, which led to a non-positive definite Hessian matrix. Based on preliminary fits, several of the selectivity and retention parameters were consequently pre-specified (Supplementary Table A.4).

Supplementary Appendix A outlines the likelihood function that is maximized to obtain the values for the parameters of the population dynamics model. The values for fecundity- and weight-at-length are set based on the outcomes of auxiliary studies, and natural mortality is set to the values used in assessments (Supplementary Table A.2).

The values for h and R_0 are chosen so that under deterministic considerations and in the absence of the effects of ocean pH (i.e., $\Omega = \Delta = 1$; σ_R=0), F_{MSY}=$F_{35\%}$ by stock and the recruitment at $\text{MMB}_{35\%}$ is the average of the estimates of recruitment over 1998 to 2019 (i.e., ignoring the recruitment estimates for the first and last years included in the analysis). The value of h for a stock is selected so the derivative of the equilibrium catch with respect to the fully-selected fishing mortality for the fleet that targets that stock is zero at F=$F_{35\%}$ when fishing mortality for the fleets that take the stock as bycatch are set to $F_{35\%}$[5]. The assumption that F_{MSY}=$F_{35\%}$ is commonly made when conducting projections for North Pacific crab and groundfish stocks (e.g., Punt et al., 2012). Punt et al. (2014b) show that the assumption F_{MSY}=$F_{35\%}$ is supported for several North Pacific crab stocks.

[5] Note that this does not imply that the derivative of the total (over stocks) catch with respect to fully-selected fishing mortality is zero at $F_{35\%}$.

2.3 Impacts of ocean acidification on pre-recruitment dynamics

As in Punt et al. (2014a, 2016, 2020), a stage-structured pre-recruitment model was used to forecast the changes over time in recruitment to the first size-class in the post-recruitment model (25-45 mm carapace width, CW for snow and southern Tanner crab and 65-80mm carapace length for red king crab):

$$\underline{N}_{T+t+1} = \mathbf{G}_T \mathbf{\Omega}_T \underline{N}_{T+t} \quad (8)$$

where $\underline{N}_{T+t}$ is the vector of numbers-at-stage at time $T+t$ (embryos enter the first stage when they are spawned), $\mathbf{G}_T$ is the growth transition matrix (i.e., the matrix of probabilities of growing from one stage to each other stage for embryos spawned at time T), and Ω_T is the survival matrix for embryos spawned at time T. The last stage in this model was the first size-class in the post-recruitment model from which the quantities Δ_y and P_y are computed. The pre-recruitment model can be used to compute the probability of surviving from entering a stage (e.g., the embryo or first juvenile stage) to entering any later stage and the expected time for this transition to take place.

As in Punt et al. (2014a; 2016, 2020), the time-step for the pre-recruit model [6 days] was set so that the time-step is able to match the durations of each stage relatively closely and it was assumed that all individuals within a stage were subject to the same survival probability and stage duration, and individuals must stay in a stage for a defined minimum amount of time before progressing to the next stage. This was achieved by dividing each of the stages into sub-stages where the number of sub-stages was one plus the number of time-steps that an animal needs to remain in a stage (Punt et al., 2014a; Supplementary Appendix D). The values of the parameters of $\mathbf{G}_T$ **(**$S_{i,T}$**,** the probability of survival for stage i for animals spawned at time T, and $P_{i,T}$, the probability of growing out of stage i for animals spawned at time T) were solved to match values for expected survival predicted from the equations based on experimental data (Supplementary Appendix B). The survival and growth of larval stages were related to surface temperature and that of juveniles to bottom temperature.

Projections of environmental variables for Bristol Bay and the eastern Bering Sea were derived from the gridded (1° latitude x 1° longitude) monthly global model projections for sea surface temperature and sea surface pH spanning 2006-2100 from the GFDL-ESM2M model (Dunne et al., 2013) under the RCP8.5 emission scenario from the 5th phase of the Coupled Model Intercomparison Project (CMIP5) (Taylor et al., 2012). Ratios of average summer sea bottom temperature to average summer sea surface temperature were calculated from the

Eastern Bering Sea Continental Shelf Trawl Survey, for the years 2017-2019. These ratios were applied to the sea surface temperature projection to make a gridded projection for sea bottom temperature. A trawl survey station was selected for each crab species based on local conditions conducive to larval settlement and juvenile growth.

For red king crab, shallow areas in Bristol Bay are conducive to settlement and growth (Daly et al., 2020; McMurray et al., 1984; Wainwright et al., 1992). Station K-14 is the shallowest/warmest station in Bristol Bay, with depth recordings of 24-26m, and a survey average sea surface temperature of 7.9°C (maximum: 9.4°C) vs. the 2017-19 projection average of 8.1°C (maximum: 8.8°C) for the 1°x1° grid cell that contains station K-14 (i.e., 58°-59° latitude and 159°-160° longitude). The ratio at station K-14 of survey average sea bottom temperature over survey average sea surface temperature was applied to make a sea bottom temperature projection spanning 2006-2100. Thus, the 2017-19 summer average for this sea bottom temperature projection, 6.7°C, exactly matches the survey average at station K-14 (maximum: 7.3°C vs. 7.0°C, respectively).

For snow crab, the cold pool in the middle domain of the Bering Sea is suitable for settlement, and station N-22, which is contained in a 1°x1° grid cell southeast of St. Matthew Island (i.e., 59°-60° latitude and 171°-172° longitude), with depth recordings of 87-88m, lies approximately on the axis of the cold pool that shows the average position of the summer sea bottom temperature divide (Fig. 5 of Parada et al., 2010). The sea surface temperature projections southeast of St. Matthew Island for 2017-19 are colder than the survey sea surface temperatures. Consequently, the ratio at station N-22 of average sea bottom temperature over average sea surface temperature was applied for the sea bottom temperature projection to the sea surface temperature projection from a 1°x1° grid cell (i.e., 59°-60° latitude and 163°-164° longitude) with a projection average sea surface temperature for 2017-19 of 8.5°C (maximum: 9.2°C) vs. survey average sea surface temperature of 9.0°C (maximum: 10.0°C) at station N-22. The 2017-19 summer average for this sea bottom temperature projection, 1.8°C, exactly matches the survey average at station N-22 (maximum: 2.0°C vs. 3.1°C, respectively).

For southern Tanner crab, juveniles were observed concentrated north of the Alaska Peninsula and near Unimak Pass (Figure 4(A) of Ryer et al., 2016), with relatively warm sea bottom temperatures. Station Z-05 is the closest station to Unimak Pass, the shallowest/warmest station in this area, with recorded depths of 83-85m, and a survey average sea surface temperature of 7.4°C (maximum: 7.9°C) vs. the 2017-19 projection average of 6.8°C (maximum: 7.3°C) for the 1°x1° grid cell that contains station Z-05 and Unimak Pass (i.e., 54°-55° latitude and 165°-166° longitude). The ratio at station Z-05 of survey average sea bottom temperature over survey average sea surface temperature was applied to make a projection of sea bottom temperatures spanning 2006-2100. Thus, the 2017-19 summer average for this sea bottom temperature projection, 5.9°C, exactly matches the survey average at station Z-05 (maximum: 6.3°C vs. 6.1°C, respectively).

2.4 Economic submodel

The profit during year y is given by:

$$\pi_y = \sum_f (\sum_s p^s C_y^{\mathrm{D},s,f} - c^f E_y^{D,f}) \tag{9}$$

where p^s is the real price per ($/t) for stock s (assumed to be time-invariant), c^f is the cost per unit effort for fleet f (Supplementary Table E.1), and $E_y^{\mathrm{D},f}$ is the number of days fishing by directed (D) fleet f during year y, computed as $q^{*,f} F_y^{\mathrm{ref},f}$ where q^{*f} is computed from a linear regression of $E_y^{\mathrm{D},f}$ on $F^{\mathrm{ref},f} e^{\eta_y^f}$ (Supplementary Fig. 1; Supplementary Table E.3). Cost includes daily-equivalent expenditures for vessel capital, labor, bait, food, and fuel (Supplementary Table E.1; Supplementary Figs E.1, E.2, and E.3).

2.5 Reference points and projections

2.5.1 Reference points

Four reference points are computed:

(1) $F_{35\%}$, the proxy for F_{MSY} for Tier 3 stocks (NPFMC, 2008);

(2) F_{MSY}, the time-invariant fully-selected fishing mortality (by fleet) that maximizes the sum of the catches over all stocks in equilibrium;

(3) F_{MEY}, the time-invariant fully-selected fishing mortality (by fleet) that maximizes Equation 9 in equilibrium; and

(4) F_{opt}, the annually varying fully-selected fishing mortality (by fleet) that maximizes the discounted (annual discount rate of 5%) sum of Equation 9.

Three stocks are modelled so the reference points are vectors (matrices for F_{opt}) with one element (vector) for each of snow, red king and southern Tanner crab and the calculation of the reference points assumes perfect information about the population dynamics and the effects of temperature and ocean pH. The reference points $F_{35\%}$, F_{MSY}, and F_{MEY} are computed for a reference period (2006-2019) and each year from 2020 to 2100. This annual calculation assumes that the population is in equilibrium with respect to temperature and ocean pH in the given year. Note that F_{MSY}, and F_{MEY} and F_{opt} are computed in equilibrium and for the temperature and ocean pH for a single year, whereas F_{opt} integrates over the entire time-series of temperatures and ocean pHs from 2020 to 2100. F_{MEY} and F_{opt} also differ in that fishing mortality varies among years (2020-2080) for F_{opt} but is time-invariant for F_{MEY}. The fully-selected fishing mortalities for 2081-2100 are set to those for 2080 when calculating F_{opt} to avoid "end effects" whereby fishing mortality is increased markedly at the end of the (finite) projection period.

F_{opt} is computed (a) under deterministic conditions (no variation in recruitment about the stock-recruitment relationship, i.e. σ_R=0.6 in Equation 7) and (b) when allowance is made for stochastic variation in recruitment about the stock-recruitment relationship (σ_R=0.6; 100 replicate projections). The annual varying fully-selected fishing mortalities are selected in the latter case to maximize the expected value (over the 100 replicate projections) of the discounted sum of profits.

2.5.2. Projections

Deterministic and stochastic projections (with annually varying values for Ω_y and Δ_y) are undertaken to explore the performance of various harvest control rules:

(1) $F_{35\%}$ computed for the reference period;
(2) F_{MSY} computed for the reference period;
(3) F_{MEY} computed for the reference period;
(4) F_{opt} based on deterministic projections;
(5) F_{opt} based on stochastic projections;
(6) the average fishing mortality rates by stock during the 2010/11-2019/20 fishing seasons;
(7) the Acceptable Biological Catch control rule, which annually sets a catch limit based on a pre-specified fraction (default 0.75; Anon, 2020[6]) of the OFL. The OFL is computed using the fishing mortality rate determined from the Tier 3 harvest control rule (NPFMC, 2008):

$$F_y^D = \begin{cases} 0 & \text{if } MMB_y / MMB_{\text{ref}} < \beta \\ F_{\text{ref}}(MMB_y / MMB_{\text{ref}} - \alpha)/(1-\alpha) & \text{if } \beta \le MMB_y / MMB_{\text{ref}} < 1 \\ F_{\text{ref}} & \text{if } MMB_y / MMB_{\text{ref}} \ge 1 \end{cases} \quad (11)$$

[6] The most recent buffers between OFL and ABC are 50%, 20% and 25% for EBS snow crab, EBS southern Tanner crab and Bristol Bay red king crab but 25% is closer to the long-term average.

where MMB_{ref} is the reference mature male biomass (corresponding to $F_{35\%}$), and α and β are control rule parameters (with default values of 0.1 and 0.25 respectively; NPFMC (2008)). Note that F_y^D depends on MMB_y through Equation 11, which itself depends on F_y^D; hence Equation 11 needs to be solved iteratively.

The results of the projections are summarized by (a) the average total catch over the projection period (2020-2100), (b) the average total revenue over the projection period, (c) the average total cost over the projection period, (c) the average profit over the projection period, (e) the discounted sum of profits over the projection period, and (f) the ratio of the mature male biomass at the end of the projection period to the unfished mature male biomass based on the reference period.

2.5.2.1 Approximately optimal harvest control rules

The harvest control rule rule F_{opt} (whether computed from deterministic or stochastic projections) involves changing the target fishing mortality each year, but is based on fully-selected fishing mortalities computed based on a projection starting in 2020. Unlike the ABC control rules, F_{opt} consequently does not take account of the estimate of stock size in the year concerned when selecting the target fishing mortality. A series of alterative harvest control rules based on the ABC control rule that vary α, β and the buffer between the ABC and the OFL were therefore explored using stochastic projections.

3. Results

3.1 Multi-species stock assessment with technical interactions

The model fits the available data sources adequately. It matches the observed landings almost exactly and mimics the size composition of the landings well on average (Supplementary Fig. 2), although there is among-year variation in the fit to the catch size-compositions (results not shown). The model is generally able to mimic the trends in the bycatch of the three stocks in the fisheries that target each stock (Supplementary Fig. 3) and their size-composition (Supplementary Fig. 4). The fits to the bycatch data are, however, notably more noisy given that the fishing mortality rates that lead to bycatch are based on those that determine the landed catches (Eqn 4) and the lesser weight applied to the bycatch data (Supplementary Table A.3).

The fits to the survey biomass index data (Fig. 3, left panels) capture the trends well, in particular a recent increase in the biomass of EBS snow crab[7] (Fig. 3a), and recent declines in the biomass of EBS southern Tanner crab and Bristol Bay red king crab (Figs 3b,c). The model does not capture the occasional outliers for southern Tanner crab during the period of higher biomass between 2006-08 and 2013-14. The survey size-composition data (aggregated over year) are mimicked adequately, at least on average (Figs 3d-f).

The trends in mature male biomass mimic those in survey biomass (Fig. 3, left panels; Fig. 4, upper panels) while recruitment is variable over time with occasional strong year-classes (except for Bristol Bay red king crab, which has experienced a period of below average recruitment for about a decade) (Fig. 4, center panels). Fishing mortality (Fig. 4, lower panels) for EBS snow crab and Bristol Bay red king crab are driven primarily by the target fishery (solid lines). In contrast, technical interactions caused by targeted fishing for EBS snow crab and Bristol Bay red king crab are substantial and consequential for EBS southern Tanner crab, with fishing mortality due to targeted fishing only exceeding that due to bycatch during the 2013-14, 2014-15, 2017-18 and 2018-19 fishing seasons. The estimates of mature male biomass for the three stocks have the same temporal pattern and scale as the estimates from the baseline models from the most recent assessments (Szuwalski, 2020 for EBS snow crab; Stockhausen, 2020 for EBS southern Tanner crab; Zheng and Siddeek, 2020 for Bristol Bay red king crab; Supplementary Fig. 6) even though the post-recruitment model of this paper differs somewhat from the models on which the most recent assessments are based and the assessment model of this paper does not consider all the data sources used in the actual assessments.

3.2 Impact of temperature and pH on growth and survival

The temperature and pH encountered by crab differ by stock and stage (Supplementary Fig. 7, left panels). Temperature exhibits an increasing trend during 2020-2100, but there is considerable among-year variability and the average temperature experienced by pre-recruit crab depends on stage, with temperature for the bottom-dwelling juvenile stages lower (and generally less variable) than for the surface-associated larval stages. Ocean pH declines over time, and there is lesser inter-annual and among-stage variability (Supplementary Fig. 7, right panels).

[7] This analysis does not use the most recent (2021) data for EBS snow crab which suggest a decline in abundance, perhaps related to increased natural mortality.

The pre-recruitment model estimates the survival from the embryo stage to the first size-class in the post-recruit model and the time to grow from the embryo stage to that size-class. Generally, higher temperature leads to lower daily survival and faster growth while lower pH leads to lower survival and slower growth rates. There is a declining trend in survival for Bristol Bay red king cab (Fig. 5, dotted lines) but with considerable inter-annual variability. In contrast, survival for EBS southern Tanner crab declines smoothly over time, while survival for EBS snow crab increases over time but with variability (Fig. 5, dashed and solid lines, respectively). The differences in results among stocks are due to whether and how temperature and pH impact growth and survival (Supplementary Appendix B). For example, both temperature and pH impact survival and growth of larval (Z1-Z4) and early juvenile (C1-C8) stages of red king crab while only pH impacts growth and survival of juvenile (C1-C8) southern Tanner crab. Survival for snow crab increases because increasing temperature increases the growth rate of larval (stages Z1 and Z2) snow crab, which leads to higher survival owing to larvae spending less time in the low survival stages (Supplementary Fig. 8). The stage-specific effects of temperature and pH (Supplementary Fig. 7) illustrate the diversity of the effects (and the experiments that have been conducted)[8].

3.3 Yield analysis (average 2006-2019)

Fig. 6 shows the base yield analysis (no landing of crab caught as bycatch) when environmental conditions are set to the average over 2006-2019 (the reference period) (see Supplementary Fig. 9 for the case when landing of retained-size crab occurs in all fleets). The reference period is used to define $F_{35\%}$, the vector of fully-selected fishing mortality rates at which spawning biomass-per-recruit (here MMB-per-recruit) is reduced to 35% of its unfished level (Fig. 6a, black lines). Note that the intercept on the ordinate is not 1 because the lines on Fig. 6a involve changing the fishing mortality for one fleet, fixing the fishing mortalities for the remaining fleets at $F_{35\%}$. $F_{35\%}$ is 1.55, 0.68, and 0.31yr^{-1} for EBS snow crab, EBS southern Tanner crab and Bristol Bay red king crab, respectively. These values are 3.5, 25.8, and 1.4 times recent average fishing mortality rates over the last ten years, which is not unexpected given the TACs set by the Alaska Department of Fish and Game (ADF&G) are often substantially less than the catches corresponding to $F_{35\%}$ (see, for example, Anon, 2020), and because the fishery for EBS

[8] There is an upper limit on the extent to which stage duration increases for EBS southern Tanner crab and Bristol Bay red king crab because although pH drops below 7.5, the experiments did not consider values lower than 7.5 so the effect of pH on growth was constrained to that for a pH of 7.5.

southern Tanner crab has been closed several times during the last 10 years (Stockhausen, 2020).

The values for the steepness of the stock-recruitment relationship (assumed not to be impacted by ocean pH) are selected so that F_{MSY}=$F_{35\%}$ are 0.726, 0.679, and 0.712 for EBS snow crab, EBS Tanner crab and Bristol Bay red king crab, respectively (see Supplementary Fig. 10 for the inferred stock-recruitment relationships). The equilibrium MMB when F=F_{MSY}, expressed as a proportion of unfished MMB is consequently less than 0.35 (0.282, 0.263 and 0.277 for EBS snow crab, EBS southern Tanner crab and Bristol Bay red king crab, respectively, Fig 6a). The total catch achieves its maximum when the directed fishing mortalities are 1.26, 0.39 and 0.31yr^{-1} for EBS snow crab, EBS southern Tanner crab and Bristol Bay red king crab, respectively. These values differ from those for $F_{35\%}$ because maximizing total catch is not the same as individually maximizing the catch (contrast Figs 6b and 6c). The shape of the yield function differs among species, with that for EBS snow crab quite flat and that for Bristol Bay red king crab quite peaked (Fig. 6b). This difference arises because the selectivity pattern for EBS snow crab is more shifted to larger animals compared to the maturity-at-length pattern than is the case for Bristol Bay red king crab. The total yield curve (Fig. 6c) is flatter than the yield curves by species (Fig. 6b).

The fully-selected fishing mortality rates by fleet at which total profit is maximized, F_{MEY}, differs markedly among species (0.50, 0.01 and 0.19 yr^{-1} for EBS snow crab, EBS southern Tanner crab and Bristol Bay red king crab), and are markedly lower than the fully-selected fishing mortality rates corresponding to MSY. The extremely low F_{MEY} value for southern Tanner crab (0.01yr^{-1}) is explained by the large estimated differences between species in fishing mortality per unit fishing effort seen in Supplementary Fig. 1 where 1,000 days of fishing effort leads to a fishing mortality rate of about 0.2 yr^{-1} for snow crab, but only about 0.05 yr^{-1} for southern Tanner crab. This relationship is reflected in Figs 6d-f, which show that changing the fully-selected fishing mortality for the EBS southern Tanner fleet has relatively small effects on total revenue, total catch and total profit. As expected, MEY does not occur at the point at which revenue is maximized (Fig. 6d). The relationship between total revenue and total profit are largely independent of the fishing mortality for EBS southern Tanner crab because given the lower value for F_{MEY} for this stock (0.01yr^{-1}), increasing it by a factor of 4 has a negligible impact on the population dynamics and hence yield and revenue.

3.4 Impact of climate change on reference points

Fig. 6 and Supplementary Fig. 9 were based on setting the temperature and pH to the averages over 2006-2019. Fig. 7 shows how F_{MSY} / MSY and F_{MEY}/profit change over time when all bycatch is discarded. The results in Fig. 7 reflect the values for the reference points when temperature and ocean pH are set for each year from 2020 to 2100 rather than to the values for the average temperature / pH over 2006-2019. F_{MSY} and F_{MEY} for EBS snow crab from 2020 are generally higher than for the reference period because the model for EBS snow crab only involves temperature-related reductions in the duration of the larval stage, which increases survival through the larval stage.

The values of year-specific F_{MSY} for Bristol Bay red king crab for 2020-2100 are generally larger than F_{MSY} for the reference period (Fig. 7a) but the year-specific MSY is less than that for the reference period. In contrast, F_{MEY} is a declining function of time for Bristol Bay red king crab (Fig. 7c). This arises because MSY drops over time with (generally) higher fishing mortality (and hence cost). Consequently, profit is maximized at increasingly lower levels of fishing mortality over time. F_{MSY} and MSY for EBS southern Tanner crab decline over time (Figs. 7a,b) whereas F_{MEY} is essentially zero for the entire period 2020-2100. The maximum profit declines over time primarily due to a reduction in the profit from the fishery for Bristol Bay red king crab (and to a much lower extent that for EBS southern Tanner crab, which is relatively low even in the reference period).

3.5 Harvest control rules

The results in Fig. 7 illustrate the impact of temperature and ocean pH on productivity, but are somewhat unrealistic because they reflect an equilibrium situation (of temperature and ocean pH and of recruitment about the stock-recruitment relationship). The calculations on which Fig. 7 are based also assume perfect information about stock status, temperature and ocean pH such that fishing mortality can be selected to achieve a management goal. Moreover, apart from the two "optimal" harvest control rules, they are based on a static harvest control rule (i.e., based on values for reference points computed for the reference period [Fig. 4]). The projections used to compare harvest control rules account for uncertainty in recruitment about the stock-recruitment relationship.

3.5.1 Deterministic projections

Table 1 compares the summary statistics for five harvest control rules but σ_R=0 and all bycatch is discarded. Results are shown for projections in which survival and growth are driven by environmental factors and in which survival and growth remain at thier reference levels. As expected, fishing at F_{MSY} leads to higher total catches than fishing at $F_{35\%}$ but the difference is not marked (~1.6%), a result expected from Fig. 6. Fishing at F_{MEY} leads to lower yields and revenue but substantially lower costs and hence higher profits. Fishing at recent average levels leads to similar outcomes to fishing at F_{MEY} but the F_{MEY} harvest control rule leads to greater average and discounted profits. The F_{opt} harvest control rule, which sets fully-selectivity fishing mortality rates by year and fleet to maximize discounted profit (Fig. 8) leads (by construction) to higher profits than the other harvest control rules and hence higher discounted profits. The $F_{35\%}$ and F_{MSY} harvest control rules lead to the MMB at the end of projection period for EBS snow crab being at or above that corresponding to MSY for the reference period but to MMB for EBS southern Tanner and Bristol Bay red king crab well below these levels (compare the values in parentheses with those not in parentheses). The F_{MEY}, Recent F and F_{opt} harvest control rules all lead to higher levels of MMB at the end of the projection period than the $F_{35\%}$ and F_{MSY} harvest control rules, but not as high as the MMB corresponding to MSY for the reference period. All harvest control rules lead to very low levels of MMB for Bristol Bay red king crab, although even setting fishing mortality by fleet to zero leads to MMB at the end of projection period for this stock that 14.9% of the unfished MMB in the reference period (the corresponding values for EBS snow and EBS southern Tanner crab are 103.5% and 22.1%). In general projections that account for the impact of environmental impacts on pre-recruitment dynamics lead to less optimistic results (lower catches and incomes and particularly profits) , with the effects most marked for $F_{35\%}$ and F_{MSY} harvest control rules.

The results are not markedly impacted by landing of some bycatch (the crab that would be retained had they been caught in a directed fishery) (Table 2), although profits for the F_{MEY} (and particularly) the F_{MSY} harvest control rules are higher, the latter mainly because the costs needed to obtain similar catches are lower. The final stock size for the F_{MSY} harvest control rule is also higher when some bycatch can be landed.

3.5.2 Stochastic projections

The stochastic projections are summarized by distributions (medians, 50% and 90% intervals) for the seven summary statistics. Fig. 9 compares the summary statistics for nine harvest control rules, the five included in Table 1, the variant of F_{opt} harvest control rule that selects fully-selected fishing mortality by fleet and year accounting for variation in recruitment about the stock-recruitment relationship ($F_{\mathrm{opt\text{-}sto}}$), and ABC control rules based on target fishing mortality rates of $F_{35\%}$, F_{MSY} and F_{MEY}. The results of the stochastic projections are broadly comparable with those of deterministic projections in Table 1. Notwithstanding leading to highly variable time-trajectories of fishing mortality by stock (Fig. 8), $F_{\text{opt-sto}}$ only leads to a discounted total that is 0.2% larger than $F_{\text{opt-det}}$ (in terms of means across simulations). The harvest control rules that include the ABC control rule (F-ABC$_{35\%}$, F-ABC$_{MSY}$, F-ABC$_{MEY}$) lead to the higher (albeit still low) MMB for Bristol Bay red king crab at the end of the projection period. Of these harvest control rules F-ABC$_{MEY}$ leads to a (mean across simulation) discounted total profit that is 92% of $F_{\text{opt-sto}}$, but to an MMB for Bristol Bay red king crab that is 36% larger than for $F_{\text{opt-sto}}$ (see Supplementary Fig. 11 for detailed results).

3.5.3 Approximately-optimal harvest control rules

The approximately-optimal harvest control rules are based on the F-ABC$_{MEY}$ harvest control rule as F-ABC$_{MEY}$ achieved near optimal discounted profits and the highest MMB for Bristol Bay red king crab. The expected discounted profit based on stochastic projections is greater than that achieved by the F-ABC$_{MEY}$ harvest control rule (median and lower 5th percentile) for higher values for the multiplier applied when computing the ABC (contrast the results for a multiplier of 1.05 to those for a multiplier of 0.75; rows 4 and 2 of Fig. 10). The highest discounted total profits occur for a harvest control rule that is more aggressive in terms of how much the target fishing mortality is reduced when the stock is below $B_{35\%}$ (α > 0.8; β ~0.5). Adopting a higher value for β also leads to better conservation outcomes for Bristol Bay red king crab, with the highest lower 5th percentile for final MMB relative to MMB_0 for this stock occurring for β>0.9. However, adopting a value of β of this magnitude risks lower total discounted profits. In contrast, the current values for α and β lead to quite poor conservation performance for Bristol Bay red king crab without an appreciable economic benefit (the black circles are in the red and yellow regions of Fig. 10).

4. Discussion

Fishery management advice (both tactical and strategic) based on population dynamics models fitted to monitoring data typically ignores most aspects of EBFM, except implicitly by allowing some parameters (e.g., growth, recruitment, selectivity) to vary over time. This paper extends previous work by Punt et al. (2014, 2016, 2020) by 1) simultaneously considering three stocks and hence of the bulk of the revenue in the crab fisheries of the eastern Bering Sea, 2) by including temperature drivers of larval and juvenile survival, and 3) including the impact of temperature and ocean pH on growth rates. While ocean pH will likely slow down growth rates (Appendix C), higher temperatures will lead to faster growth.

The trends in survival to recruitment for EBS southern Tanner crab and Bristol Bay red king crab are qualitatively similar to those of previous work (Punt et al., 2014, 2016, 2020) but with greater inter-annual variation owing to the use of a more realistic model for changes over time in temperature (bottom and surface) and ocean pH, with different trends in these environmental variables for the different stages in the model.

The fishing mortality rates at which profit is maximized decline over time (albeit with considerable inter-annual variation) for Bristol Bay red king crab while this is not the case for the fishing mortality at which yield is maximized for this stock and those at which yield and profit are maximized for EBS snow crab. The results for Bristol Bay red king crab arise because the yield corresponding to MSY declines over time (Fig. 7d), but the cost corresponding to MSY is constant over time if the F_{MSY} is constant over time, leading to increasingly lower (and often negative) profits over time. Consequently, F_{MEY} occurs at a lower level of fishing mortality over time given that costs decline linearly with reductions in fishing mortality while yield declines more slowly than declines in fishing mortality (Fig. 6d,e).

The results for EBS southern Tanner crab suggest that F_{MEY} is near zero for this species (Fig. 7). This arises because EBS southern Tanner crab is bycatch in the other directed fisheries and the fishery for southern Tanner crab also leads to bycatch of other species. Overall, a greater total profit can be obtained by avoiding the bycatch due to fishing for EBS southern Tanner crab even though there is value in terms of yield in a directed fishery for EBS southern Tanner crab (contrast Figs 7c and 7a).

A harvest control rule that sets fishing mortality for each directed fishery to F_{MEY} leads, as expected, to the highest profits, with harvest control rules that set annual fishing mortality rates to maximize total profits (the F-opt harvest control rules) only leading to marginally greater profits even though such harvest control rules would lead to a much more complex management system (Fig. 8). The F_{MEY} harvest control rule leads, as expected, to lower yields than the F_{MSY} and $F_{35\%}$ harvest control rules, but not to the extent to which it leads to higher profits. This is again not unexpected given the nature of the relationship between yield and cost as a function of fishing mortality.

Most previous evaluations of bioeconomic strategies, including those of Punt et al. (2014, 2016, 2020) evaluated harvest control rules in which fishing mortality was constant over time and independent of biomass. However, in actuality, most of the harvest control rules used when providing management advice are of the threshold type where fishing mortally is reduced when population biomass is below a given management reference point (Deroba and Bence, 2008). For Bristol Bay red king crab, threshold strategies led to reduced profits but improved conservation compared to constant fishing mortality strategies. The conventional harvest control rules applied to crab stocks in the eastern Bering Sea set the parameters α and β (respectively, the proportion of $MMB_{35\%}$ at which the fishing mortality is set to zero and rate at which catch limits are reduced from the limit value) to 0.1 and 0.25 but the stochastic simulations indicate that higher profits can be obtained with harvest control rules that reduce fishing mortality faster when the biomass is below the threshold biomass of $MMB_{35\%}$. Such harvest control rules also provide additional protection for stocks (such as Bristol Bay red king crab) that are predicted to decline due to the effects of climate change, while also allowing fisheries on healthy stocks (in this study EBS snow crab) to continue. This study did not explore charges to the point at which fishing mortality could be reduced owing to low biomass, setting it to $B_{35\%}$ but this could be explored in further work.

This paper extends Punt et al. (2020) who estimated the effects of pH on estimates of MEY for EBS southern Tanner crab and Bristol Bay red king crab. The differences in results between this paper and Punt et al. (2020) highlight the importance of fully capturing bycatch effects when estimating MEY and that assessments of the impacts of environmental variables on future dynamics of marine resources need to as fully as possible consider all environmental factors. This is highlighted by the variability in the estimates of how survival of red king crab will change over time, which are quite smooth if only ocean pH is considered but very variable when account is also taken of changes over time in temperature (compare, for example, Fig. 7 of this paper with Fig. 7 of Punt et al. [2020]).

4.1 Caveats and future work

The projections (and calculations of reference points) are based on the unrealistic assumption that the exact population biomass is known (aka Punt et al., 2008). Future work could place the analyses in the context of a management strategy evaluation (MSE; Punt et al., 2016), which would account for uncertainty in stock status and biomass, uncertainty associated with future oceanographic conditions, and uncertainty related to the impact of environmental variables on survival and growth. A MSE could also evaluate the impact of the generally more conservative Alaska Department of Fish and Game harvest control rules (e.g., Heller-Shipley et al., 2021) and/or harvest control rules that vary rates of incidentally retained catch. However, the results of this paper allow managers to compare many management options (e.g., Fig. 10) so that a subset could be explored in subsequent MSE analyses.

The analyses of this paper are focused on the direct impacts of ocean acidification and temperature using models parameterized based on experiments conducted for larval and juvenile crab. The use of variables for which the link between pre-recruitment dynamics and environmental variables is based on experimental results is more likely to lead to robust results given alternative approaches such as correlating assessment outputs with environmental variables is often subject to the possibility of spurious correlation. However, the restriction to environmental variables for which impacts on pre-recruitment dynamics can be quantified using experimental results limits the analysis because temperature and pH are not the only environmental factors subject to climate change that could be impacting EBS snow, EBS southern Tanner and Bristol Bay red king crab. For example, Szuwalski et al. (2021) examined whether environmental variables led to improved fits to recruitment estimates for these stocks and found that stock-recruitment models for EBS snow crab could be improved by including ice cover and the Arctic Oscillation (AO) as covariates while bottom temperature and cod biomass led to improved fits for EBS southern Tanner crab. None of the environmental variables considered by Szuwalski et al. (2021) led to an improvement in Akaike Information Criterion for recruitment of Bristol Bay red king crab in excess of 2. Szuwalski et al. (2021) also examined the impact of environmental variables on the centroids of abundance and the distributional extent for these three crab stocks, and found that latitude and longitude of abundance for EBS snow crab was related to the AO and to Sea Surface Temperature (SST), while the longitude of the centroid of abundance for EBS southern Tanner crab was related to SST and cod biomass. SST was found to be related to the distributional extent of Bristol Bay red king crab while ice cover and AO significantly improved the explained variability in latitude and bottom temperature and cod biomass for longitude for this stock. As the association between southern Tanner crab and Pacific cod suggests, OA, temperature, or other environmental variables could have indirect effects on crabs by changing the abundance and distribution of either predator or prey species.

Overall, Szuwalski et al. (2021) found that recruitment of EBS snow crab was likely to decline after ~2040 given warming temperatures while recruitment of EBS southern Tanner crab was likely to decline and that of Bristol Bay red king crab was predicted to be stable. These results are in conflict with the implications of the pre-recruitment models of this paper. This highlights that future studies should attempt to reflect as many reasons for environmentally-induced changes in the population dynamics of crab populations as can be supported by available data. For example, Punt et al. (2021) included ocean pH effects on pre-recruit survival of northern rock sole (*Lepidopsetta polyxystra*) in the eastern Bering Sea as well as the impacts of temperature on mean recruitment.

The analyses of this paper are predicated on the assumption that the overlap in distribution (and the timing of the fisheries) remain constant over time. Szuwalski et al. (2021) make predictions of how the centroids of abundance and distributional extent of the three crab stocks may change over time. In principle, distributional and associated changes over time could be used to develop a model for how the ratio of bycatch to target fishing mortality will change over time, but this will likely require a spatial model, and is hence beyond the scope of this paper.

Future work should focus on the sensitivity of the results to alternative climate scenarios and incorporate the actual stock assessment models, which include a terminal molt (for snow and southern Tanner crab), molting probabilities, and molt increments. The current models tend to overestimate the retained (preferred legal size) portion of the populations for EBS southern Tanner crab and snow crab, which may be due to the fairly simple structure of the population dynamics models used here. However, the use of stock assessment models will substantially increase the computational burden: for example, an assessment model with all three stocks will have ~500 estimable parameters. Finally, future experiments should continue to examine the impact of environmental variables on survival and growth at all life stages and species with large sample sizes.

4.2 Conclusions

We developed a framework that can be used to examine the consequences of temporal changes in temperature and ocean pH on yield and profit of multiple stocks that interact through technical interactions. The analyses integrate experimental work that incorporates effects of temperature and ocean pH on growth and survival at the larval and juvenile stages. Our results highlight that harvest control rules that aim to maximize profit lead to somewhat lower yields than those that aim to maximize yield. However, the extent to which harvest control rules that aim to maximize yield lead to proportionally lower profits than those that aim to maximize profits is even greater. Maximizing profits also has conservation benefits, which are increased when the harvest control rule is of the threshold type such that fishing mortality is reduced when biomass is below a threshold level. We found that including temperature effects on pre-recruitment survival and growth led to changes with respect to inferences regarding optimal levels of fishing mortality, which highlights the need to incorporate (to the extent possible given experimental work) as many of the environmental factors that impact pre-recruitment dynamics as possible. In relation to the fisheries of the Bering Sea, the results point to the need to further examine (e.g. using MSE) alternative forms of harvest control rule for crab stocks, especially given the likely effects of environmental changes on pre-recruitment dynamics

Acknowledgements

AEP was supported by NOAA through the NOAA Ocean Acidification Program. Two anonymous reviewers are thanked for their comments on an earlier version of this paper. This is CICOES contribution XXXX and AFSC contribution 17369. The findings and conclusions in the paper are those of the author(s) and do not necessarily represent the views of the National Marine Fisheries Service.

References

ADF&G (Alaska Department of Fish and Game). 1990. Policy on king and Tanner crab resource management. Document 90-04-FB.

Anon. 2020. Introduction to the NPFMC crab SAFE. https://meetings.npfmc.org/CommentReview/DownloadFile?p=23230f0c-a4c4-4530-ae12-efa09e5054be.pdf&fileName=C1%20BSAI%20Crab%20SAFE%20Intro.pdf.

Chilton, E.A., Foy, R. J., Armistead, C.E., 2010. Temperature effects on assessment of red king crab in Bristol Bay, Alaska. In Biology and Management of Exploited Crab Populations under Climate Change, pp. 249-263. Ed. by G. H. Kruse, G. L. Eckert, R. J. Foy, R. N. Lipcius, B. Sainte-Marie, D. L. Stram, and D. Woodby. Alaska Sea Grant, University of Alaska Fairbanks.

Coffey, W. D., Yarram, A., Matoke, B., Long, W. C., Swiney, K. M., Foy, R. J., Dickenson, G., 2017. Ocean acidification leads to altered micromechanical properties of the mineralized cuticle of juvenile red and blue king crabs. Journal of Experimental Mar. Biol. and Ecol. 495, 1-12.

Daly, B., Parada, C., Loher, T., Hinckley, S., Hermann, A.J., Armstrong, D., 2020. Red king crab larval advection in Bristol Bay: Implications for recruitment variability. Fish. Ocean. 29, 505–525.

Daly, B., Swingle, J.S., Eckert, G.L., 2009. Effects of diet, stocking density, and substrate on survival and growth of hatchery-cultured red king crab (*Paralithodes camtschaticus*) juveniles in Alaska, USA. Aquaculture 293, 68-73.

Deroba, J.J., Bence, J.R., 2008. A review of harvest policies: Understanding relative performance of control rules. Fish. Res. 94, 210-223,

Dickenson, G.H., Bejerano, S., Salvador, T., Makdisi, C., Patel, S., Long, W.C., Swiney, K M., Foy, R.J., Steffel, B .V., Smith, K.E., Aronson, R.B., 2021. Ocean acidification alters exoskeleton properties in adult Tanner crabs, *Chionoecetes baridi*. J. Exp. Biol. 224, doi:10.1242/jeb.232819.

Dunne, J.P., John, J.G., Shevliakova, E., Stouffer, R.J., Krasting, J.P., Malyshev, S.L., Milly, P.C.D., Sentman, L.T., Adcroft, A.J., Cooke, W., Dunne, K.A., Griffies, S.M., Hallberg, R.W., Harrison, M.J., Levy, H., Wittenberg, A.T., Phillips, P.J., Zadeh, N., 2013. GFDL's ESM 2 global coupled climate-carbon Earth system models. Part II: Carbon system formulation and baseline simulation characteristics. J. Clim. 26, 2247–2267.

Fedewa, E.J., Jackson, T.M., Richar, J.I., Gardner, J.L., Litzow, M.A., 2020. Recent shifts in northern Bering Sea snow crab (Chionoecetes opilio) size structure and the potential role of climate-mediated range contraction. Deep-Sea Rese. II. 181, 11.

Fulton, E.A., Punt, A.E., Dichmont, C.M., Harvey, C.J., Gorton, R., 2019. Ecosystems say good management pays off. Fish And Fish. 20, 66-96.

Garber-Yonts, B., Lee, J., 2021. Economic status of the BSAI King and Tanner crab fisheries off Alaska. https://meetings.npfmc.org/CommentReview/DownloadFile?p=84d483ac-bae8-437a-8649-bce5ff8480f3.pdf&fileName=D4%20Crab%20Economic%20SAFE.pdf

Heller_Shipley, M.A., Stockhausen, W.T. Daly, B.J., Punt, A.E., Goodman, S.E., 2021. Should harvest control rules for male-only fisheries include reproductive buffers? A Bering Sea Tanner crab (*Chionoecetes bairdi*) case study. Fish. Res. 243, 106049.

Hollowed, A.B., Holsman, K.K., Haynie, A.C., Hermann, A.J., Punt, A.E., Aydin, K., Ianelli, J.N., Kasperski, S., Cheng, W., Faig, A., Kearney, K.A., Reum, J.C.P., Spencer, P., Spies, I., Stockhausen, W., Szuwalski, C.S., Whitehouse, G.A., Wilderbuer, T.K., 2020. Integrated modeling to evaluate climate change impacts on coupled social-ecological systems in Alaska. Front. Mar. Sci. 6, 775.

Laman, E.A., Rooper, C.N., Turner, K., Rooney, S., Cooper, D.W., Zimmermann, M., 2017. Using species distribution models to describe essential fish habitat in Alaska. Can. J. Fish. Aquat. Sci. 75, 1230–1255.

Loher, T., Armstrong, D.A., 2005. Historical changes in the abundance and distribution of ovigerous red king crabs (Paralithodes camtschaticus) in Bristol Bay (Alaska), and potential relationship with bottom temperature. Fish. Ocean. 14, 292-306.

Long, W.C., Daly, B., 2017. Upper thermal tolerance in red and blue king crab: sublethal and lethal effects. Mar. Biol., 164, 162, doi:10.1007/s00227-017-3190-1.

Long, W. C., Pruisner, P., Swiney, K. M., Foy, R., 2019. Effects of ocean acidification on respiration, feeding, and growth of juvenile red and blue king crabs (Paralithodes camtschaticus and P. platypus). ICES J. Mar. Sci. 76, 1335–1343.

Long, W.C., Swiney, K.M., Harris, C., Page, H.N., Foy, R.J., 2013a. Effects of ocean acidification on juvenile red king crab (*Paralithodes camtschaticus*) and Tanner crab (*Chionoecetes bairdi*) growth, condition, calcification, and survival. PLoS ONE 8(4): e60959.

Long, W.C., Swiney, K.M., Foy, R.J., 2016. Effects of high pCO2 on Tanner crab reproduction and early life history, Part II: carryover effects on larvae from oogenesis and embryogenesis are stronger than direct effects. ICES J. Mar. Sci. 73, 836–848.

Long, W.C., Swiney, K.M., Harris, C., Page, H.N., Foy, R.J. 2013b. Effects of ocean acidification on juvenile red king crab (Paralithodes camtschaticus) and Tanner crab (Chionoecetes bairdi) growth, condition, calcification, and survival. PloS one, 8, e60959.

Marshall, K.N., Koehn, L.E., Levin, P.S., Essington, T.E., Jensen, O.P., 2018 Inclusion of ecosystem information in US fish stock assessments suggests progress toward ecosystem-based fisheries management. ICES J. Mar. Sci. 76, 1-9.

McMurray G., Vogel A.H., Fishman P.A., Armstrong D.A., Jewett S.C., 1984. Distribution of larval and juvenile red king crabs (Paralithodes camtschatica) in Bristol Bay. U. S. Department of Commerce, Outer Continental Shelf Environmental Assessment Program Final Report, 53, 267–477.

Meseck, S.L., Alix, J.H., Swiney, K.M., Long, W.C., Wikfors, G.H., Foy, R. J., 2016. Ocean acidification affects hemocyte physiology in the Tanner crab (Chionoecetes bairdi). PloS one, 11: e0148477, doi:10.1371/journal.pone.0148477.

Murphy, J.T., 2020. Climate change, interspecific competition, and poleward vs. depth distribution shifts: Spatial analyses of the eastern Bering Sea snow and Tanner crab (Chionoecetes opilio and C. bairdi). Fish. Res. 223, 105417

NMFS, 2016. NOAA fisheries ecosystem-based fisheries management road map. Silver Spring, MD.

North Pacific Fishery Management Council (NPFMC). 2008. Amendment 24. Final Environmental Assessment for amendment 24 to the Fishery Management Plan for Bering Sea/Aleutian Islands King and Tanner Crabs to Revise Overfishing Definitions. North Pacific Fishery Management Council, 605 West 4th Ave, Anchorage, AK 99501.

North Pacific Fishery Management Council (NPFMC). 2019. Bering Sea Fishery Ecosystem Plan. Anchorage, AK. https://meetings.npfmc.org/CommentReview/DownloadFile?p=c334ad33-4139-4b5a-b205-a8b7c5028562.pdf&fileName=D6%20Final%20BS%20FEP%20Jan%202019.pdf.

Parada, C., Armstrong, D.A., Ernst, B., Hinckley, S., Orensanz, J.M., 2010. Spatial dynamics of snow crab (Chionoecetes opilio) in the eastern Bering Sea-putting together the pieces of the puzzle. Bull. Mar. Sci. 86, 413–437.

Pitcher, T.J., Daniela Kalikoski, D. Short, K., Varkey, D., and Pramod, G., 2009, An evaluation of progress in implementing ecosystem-based management of fisheries in 33 countries. Mar. Pol. 33, 223-232.

Punt, A.E., Butterworth, D.S., de Moor, C.L., De Oliveira, J.A.A., Haddon, M., 2016. Management Strategy Evaluation: Best Practices. Fish and Fish. 17, 303-334.

Punt, A.E., Dorn, M.W., Haltuch, M.A., 2008. Evaluation of threshold management strategies for groundfish off the U.S.West Coast. Fish. Res. 94, 251-266.

Punt, A.E., Siddeek, M.S.M., Garber-Yonts, B., Daltan, M., Rugolo, L., Stram, D., Turnock, B.J., Zheng, J., 2012. Evaluating the impact of buffers to account for scientific uncertainty when setting TACs: Application to red king crab in Bristol Bay, Alaska. ICES J. Mar. Sci. 69, 624–634.

Punt, A.E., Poljak, D., Dalton, M.G., Foy, R.J., 2014a. Evaluating the impact of ocean acidification on fishery yields and profits: The example of red king crab in Bristol Bay. Ecol. Model. 285, 39–53

Punt, A.E., Szuwalski, C., Stockhausen, W., 2014b. An evaluation of stock–recruitment proxies and environmental change points for implementing the US Sustainable Fisheries Act. Fish. Res. 157, 28–40.

Punt, A.E., Foy, R.J., Dalton, M.G., Long, W.C., Swiney, K.M., 2016. Effects of long term exposure to ocean acidification conditions on future southern Tanner crab (*Chionoecetes bairdi*) fisheries management. ICES J. Mar. Sci. 73, 849–864.

Punt, A.E., Dalton, M.G., Foy, R.J., 2020. Multispecies yield and profit when exploitation rates vary spatially including the impact on mortality of ocean acidification on North Pacific crab stocks. Fish. Res. 225, 105481.

Punt, A.E., Dalton, M.G., Cheng, W., Hermann, A.J., Holsman, K.K., Hurst, T.P., Ianelli, J.N., Kearney, K.A., McGilliard, C., Pilcher, D.J. Veron.=, M., In press. Evaluating the impact of climate and demographic variation on future prospects for fish stocks: An Application for northern rock sole in Alaska. Deep Sea Res. II. 00, 00-00

Ryer, C.H., Ottmar, M., Spencer, M., Duffy-Anderson, J., Cooper, D., 2016. Temperature-dependent growth of early juvenile southern Tanner crab Chionoecetes bairdi: implications for cold pool effects and climate change in the southeastern Bering Sea. J. Shellfish Res. 35, 259–267.

Saint-Marie, B., Lafrance, M., 2002. Growth and survival of recently settled snow crab Chionoecetes opilio in relation to intra- and intercohort competition and cannibalism: a laboratory study. Mar. Ecol. Prog. Ser., 244:191-203.

Schirripa, M.J., Goodyear, C.P., Methot, R.M., 2009. Testing different methods of incorporating climate data into the assessment of US West Coast sablefish. ICES J. Mar. Sci. 66, 1605–1613.

Shotwell, S.K., Dorn, M., Deary, A. Fissel, B., Rogers, L., Zador, S., 2019. Ecosystem and socioeconomic profile of the walleye pollock stock in the Gulf of Alaska. Appendix 1A In Dorn, M.W., A.L. Deary, B.E. Fissel, D.T. Jones, N.E. Lauffenburger, W.A. Palsson, L.A. Rogers, S.A. Shotwell, K.A. Spalinger, and S.G. Zador. 2019. Assessment of the Walleye Pollock stock in the Gulf of Alaska. Stock assessment and fishery evaluation report for the groundfish resources of the Gulf of Alaska. North Pacific Fishery Management Council, 1007 W 3rd Ave, Suite 400 Anchorage, AK 99501. Pp. 105-151.

Siddon, E., 2020. Ecosystem status report 2020: Eastern Bering Sea. North Pacific Fisheries Management Council, Anchorage, AK. https://www.fisheries.noaa.gov/resource/data/ecosystem-status-report-2020-eastern-bering-sea.

Siikavuopio, S I., Whitaker, R.D., Saether, B.S., James, P., Olsen, B.R., Thesslund, T., Hustad, A., Mortsensen, A., 2017. First observations of temperature tolerances of adult male snow crab (*Chionoecetes opilio*) from the Barents Sea population and the effects on the fisheries strategy. Mar. Biol. Res. 13, 744-750,

Skern-Mauritzen, M., Ottersen, G., Handegard, N.O., Huse, G., Dingsør, G. E., Stenseth, N.C., Kjesbu, O.S., 2016. Ecosystem processes are rarely included in tactical fisheries management. Fish and Fish. 17, 165–175.

Stillman, J.H., Fay, S.A., Ahmad, S.M., Swiney, K.M., Foy, R.J., 2020. Transcriptomic response to decreased pH in adult, larval and juvenile red king crab, Paralithodes camtschaticus, and interactive effects of pH and temperature on juveniles. J. Mar. Biol. Assoc. UK. 100, 251-265.

Stockhausen, W.T., 2020. 2020 Stock Assessment and Fishery Evaluation Report for the Tanner Crab Fisheries of the Bering Sea and Aleutian Islands Regions. *In:* NPFMC (North Pacific Fishery Management Council). 2020. In: Stock Assessment and Fishery Evaluation Report for the King and Tanner Crab Fisheries of the Bering Sea and Aleutian Islands Region: 2020 Final Crab SAFE. September 2020. North Pacific Fishery Management Council, Anchorage. https://meetings.npfmc.org/CommentReview/DownloadFile?p=ea00fa2f-108d-4dfb-a4c3-24bc13f3f57c.pdf&fileName=C1%203%20Tanner%20Crab%20SAFE.pdf

Stoner, A.W., Ottmar, M.L., Copeman, L.A., 2010. Temperature effects on the molting, growth, and lipid composition of newly-settled red king crab. J. Exp. Mar. Biol. Ecol. 393, 138-147.

Swiney, K.M., Long, W.C., Foy, R.J., 2016. Effects of high pCO2 on Tanner crab reproduction and early life history, Part I: long-term exposure reduces hatching success and female calcification, and alters embryonic development. ICES J. Mar. Sci. 73, 825–835.

Swiney, K.M., Long, W.C., Foy, R.J., 2017. Decreased pH and increased temperatures affect young-of-the-year red king crab (Paralithodes camtschaticus). ICES J. Mar. Sci. 74: 1191-1200.

Szuwalski, C., 2020. A stock assessment for eastern Bering Sea snow crab. *In:* NPFMC (North Pacific Fishery Management Council). 2020. In: Stock Assessment and Fishery Evaluation Report for the King and Tanner Crab Fisheries of the Bering Sea and Aleutian Islands Region: 2020 Final Crab SAFE. September 2020. North Pacific Fishery Management Council, Anchorage. https://meetings.npfmc.org/CommentReview/DownloadFile?p=1461f42e-cfc0-448d-8106-ddd5d0ef517f.pdf&fileName=C1%201%20Snow%20Crab%20SAFE.pdf

Szuwalski, C., Cheng, W., Foy, R., Hermann, A. J., Hollowed, A., Holsman, K., Lee, J., Stockhausen, W., Zheng, J., 2021. Climate change and the future productivity and distribution of crab in the Bering Sea. ICES J. Mar. Sci. 78, 502-515.

Taylor K.E., Stouffer R.J., Meehl G.A, 2012. An overview of CMIP5 and the experiment design. Bull. Am. Meteorol. Soc. 93, 485–498.

Townsend, H., Harvey, C.J., deReynier, Y., Davis, D., Zador, S.G., Gaichas, S., Weijerman, M., Hazen, E.L., Kaplan, I.C., 2019. Progress on Implementing Ecosystem-Based Fisheries Management in the United States through the use of ecosystem models and analysis. Front Mar. Sci. 6, 641.

Wade, P.R., 1998. Calculating limits to the allowable human-caused mortality of cetaceans and pinnipeds. Mar. Mamm, Sci. 14,1-37.

Wainwright T.C., Armstrong D.A., Andersen H.B., Dinnel P.A., Herren D.W., Jensen G.C., Orensanz J.M., Shaffer, J.A., 1992. Coastal fisheries oceanography of the southern Bering Sea and north Aleutian Basin: Port Moller king crab studies. U. S. Department of the Interior, Report MMS 92-0040. 42 pp.

Yamamoto, T., Yamada, T., Kinoshita, T., Ueda, Y., Fujimoto, H., Yarnasaki, A., Hamasaki, K., 2015. Effects of temperature on growth of juvenile snow crabs, Chionoecetes opilio, in the laboratory. J. Crust. Biol. 35, 140-148.

Zheng, J., Siddeek, M.S.M., 2020. Bristol Bay red king crab stock assessment in fall 2020. In: Stock Assessment and Fishery Evaluation Report for the King and Tanner Crab Fisheries of the Bering Sea and Aleutian Islands Region: 2020 Final Crab SAFE. September 2020. North Pacific Fishery Management Council, Anchorage. https://meetings.npfmc.org/CommentReview/DownloadFile?p=06e93325-0336-4947-a2b9-cbf7b5db9bc8.pdf&fileName=C1%202%20BBRKC%20SAFE.pdf

Table 1. Summary of the deterministic projections (2020-2100) with temperature and pH-driven impacts on pre-recruitment dynamics when all bycatch is discarded. F_{MSY} and F_{MEY} are selected to maximize average catch and average profit respectively in the absence of temperature and pH effects on pre-recruits. F_{opt} involves selecting annual fishing mortality rates for 2020-2080 to maximize discounted profit. Results are shown for scenarios in which pre-recruitment dynamics are not impacted by temperature and ocean pH in parentheses.

	$F_{35\%}$	F_{MSY}	F_{MEY}	Recent Average F	F_{opt} (deterministic)
Average catch (‘000t)	51.7	52.5	43.7	43.1	
	(53.7)	(54.8)	(43.5)	(43.9)	46.0
Average revenue ($million)	328.6	333.8	279.2	276.9	
	(373.3)	(380.7)	(310.9)	(315.2)	291.1
Average cost ($million)	460.2	315.3	73.2	79.3	
	(460.2)	(315.3)	(73.2)	(79.3)	81.7
Average profit ($million)	-131.7	18.6	206.0	197.6	
	(-86.9)	(65.4)	(237.7)	(235.9)	209.4
Discounted profit ($million)	-1374.1	1496.4	4600.9	4435.5	
	(-871.5)	(1987.2)	(4890.2)	(4769.6)	4753.1
2100 depletion					
EBS snow crab	0.312	0.343	0.511	0.530	0.456
	(0.282)	(0.313)	(0.479)	(0.497)	
EBS Tanner crab	0.038	0.067	0.207	0.192	0.210
	(0.263)	(0.390)	(0.947)	(0.890)	
Bristol Bay red king	0.038	0.038	0.054	0.050	0.066
	(0.277)	(0.283)	(0.414)	(0.380)	

Table 2. Summary of the deterministic projections (2020-2100) with temperature and pH-driven impacts on pre-recruitment dynamics when landing of some bycatch is permitted. F_{MSY} and F_{MEY} are selected to maximize average catch and average profit respectively in the absence of temperature and pH effects on pre-recruits. F_{opt} involves selecting annual fishing mortality rates for 2020-2080 to maximize discounted profit. Results are shown for scenarios in which pre-recruitment dynamics are not impacted by temperature and ocean pH in parentheses.

	$F_{35\%}$	F_{MSY}	F_{MEY}	Recent Average F	F_{opt} (deterministic)
Average catch (‘000t)	45.1	49.6	43.5	42.3	
	(47.5)	(50.6)	(43.1)	(43.0	46.0
Average revenue ($million)	288.5	316.5	278.0	271.9	
	(333.7)	(355.1)	(308.2)	(309.9)	290.4
Average cost ($million)	428.2	271.6	70.6	79.3	
	(428.2)	(271.6)	(70.6)	(79.2)	80.7
Average profit ($million)	-139.6	44.9	207.4	192.7	
	(-94.4)	(83.5)	(237.6)	(230.7)	209.6
Discounted profit ($million)	-1671.4	1959.1	4621.1	4337.0	
	(-1186.1)	(2385.7)	(4900.6)	(4669.8)	4753.7
2100 depletion					
EBS snow crab	0.312	0.325	0.512	0.525	
	(0.282)	(0.294)	(0.480)	(0.492)	0.456
EBS Tanner crab	0.038	0.085	0.203	0.185	
	(0.263)	(0.464)	(0.933)	(0.862)	0.198
Bristol Bay red king	0.038	0.038	0.054	0.050	
	(0.277)	(0.277)	(0.414)	(0.379)	0.068

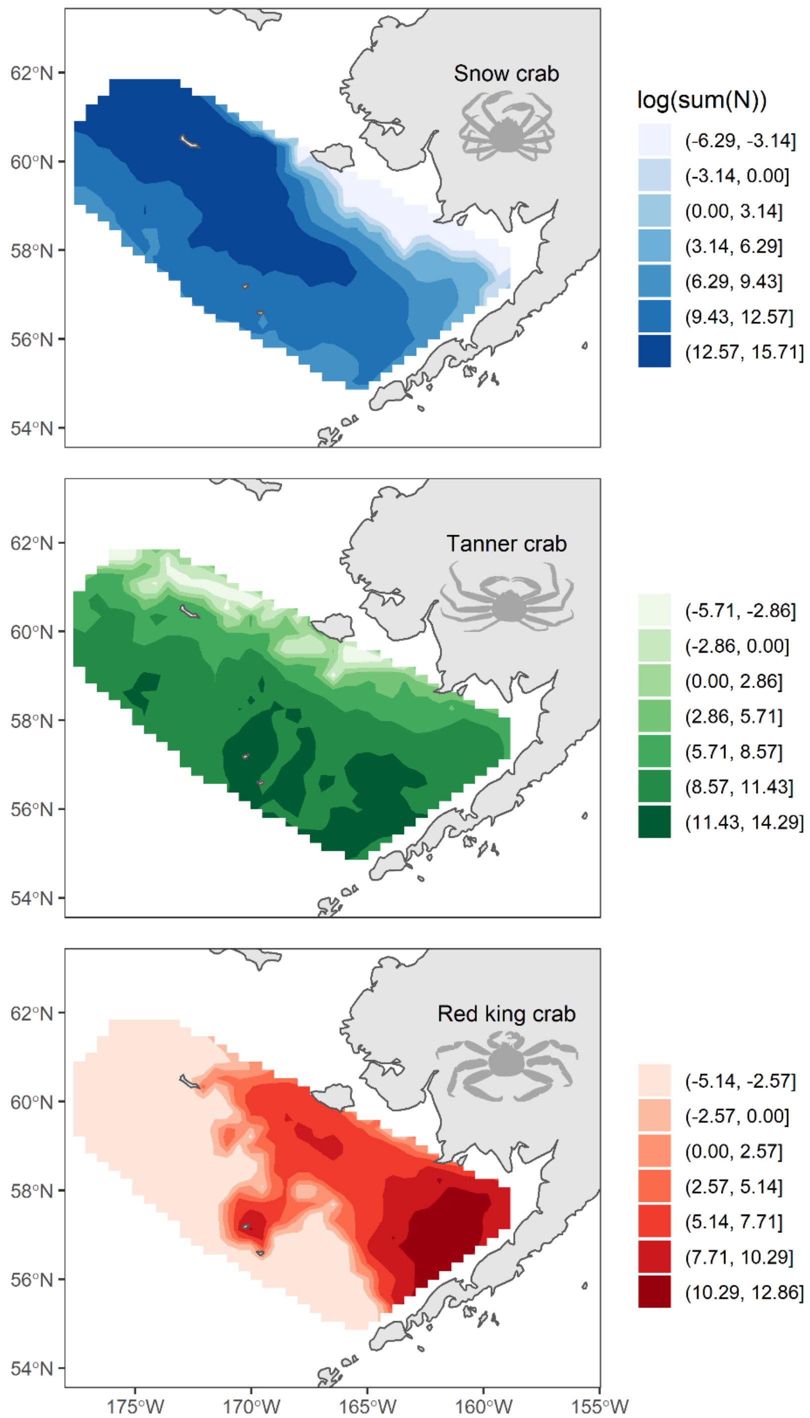

Fig. 1. Map of the Eastern Bering Sea showing the distribution areas for the three stocks considered in this paper.

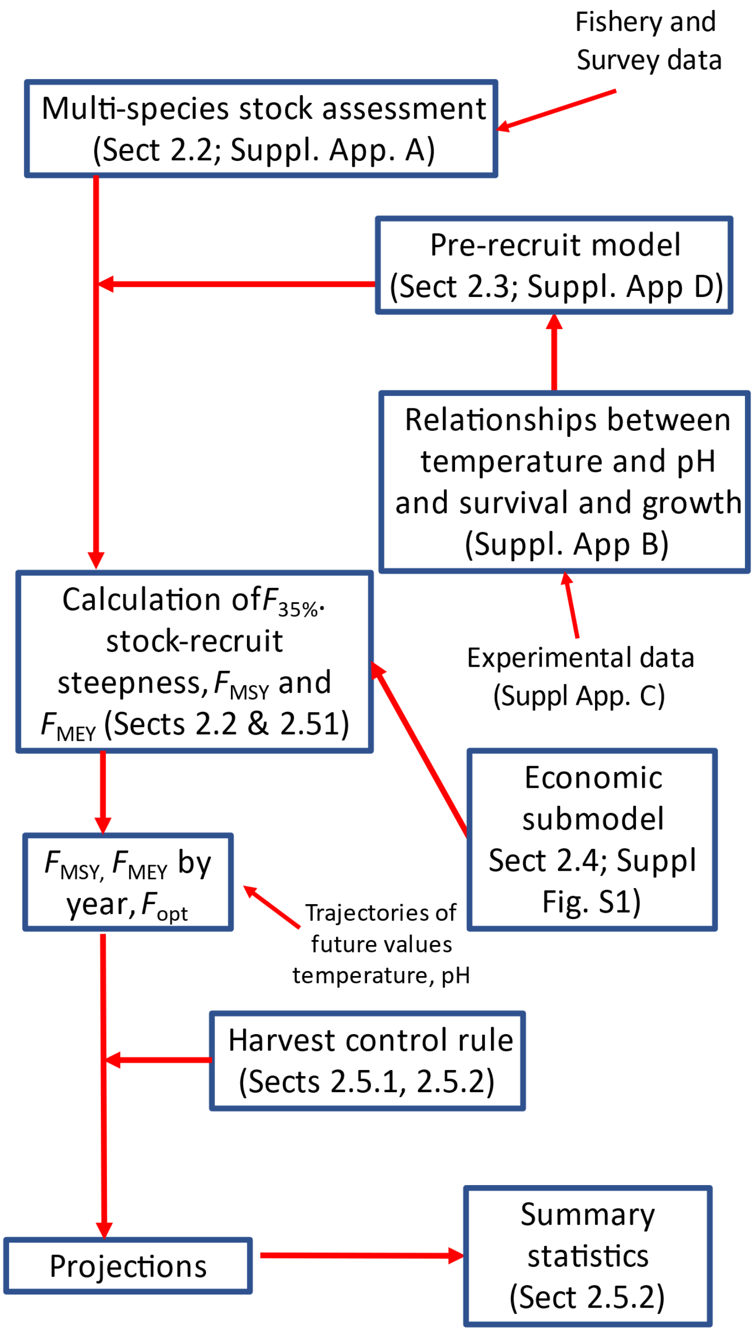

Fig. 2. Flowchart of the approach used to integrate temperature and ocean pH effects on pre-recruits and technical interactions on post-recruitments when computing reference points and conducting projections.

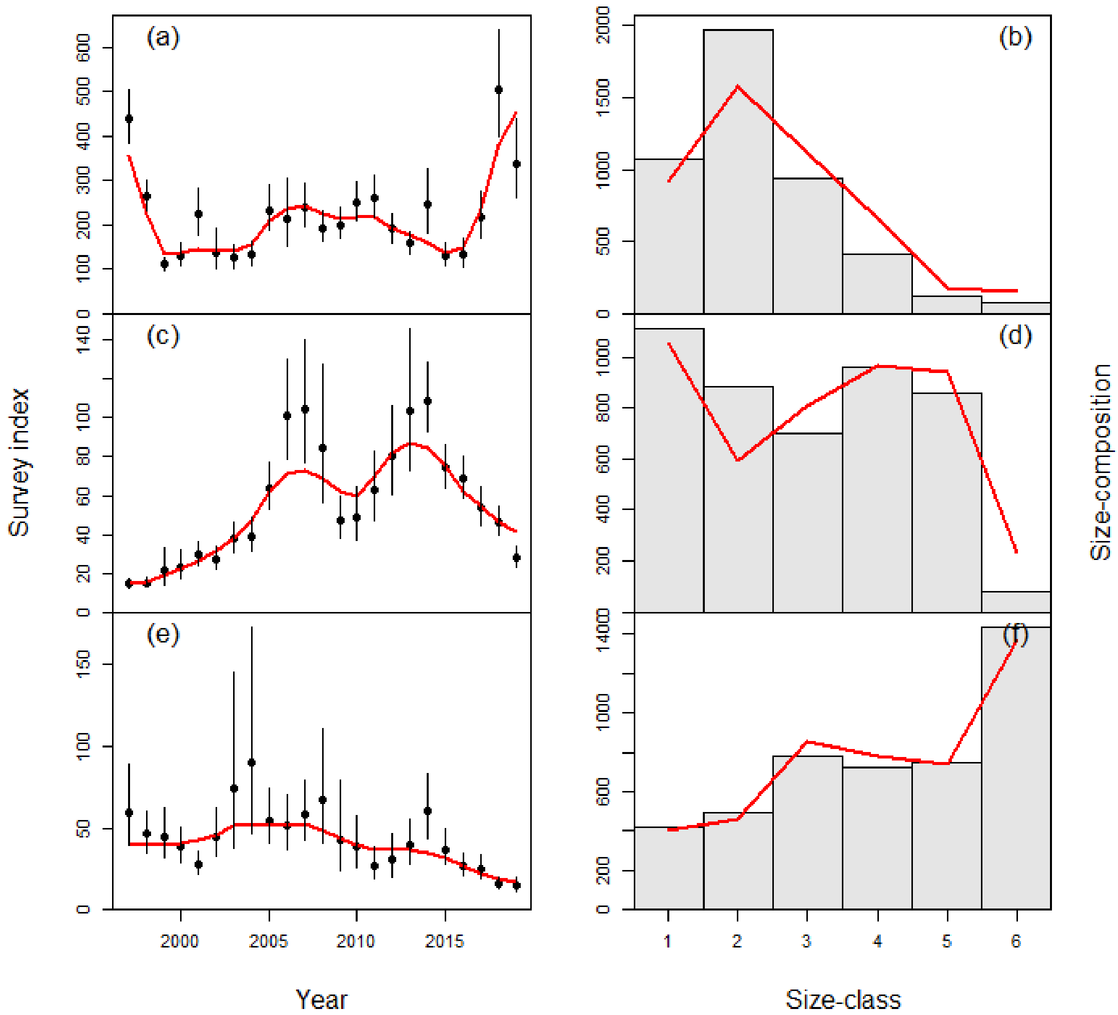

Fig. 3. Observed (dots; vertical lines denote 90% sampling intervals) and model-predicted (red lines) survey indices (left panels) and the size-composition of the survey indices aggregated over years (right panels). Results are shown for EBS snow crab (a, b), EBS southern Tanner crab (c, d), and Bristol Bay red king crab (e, f).

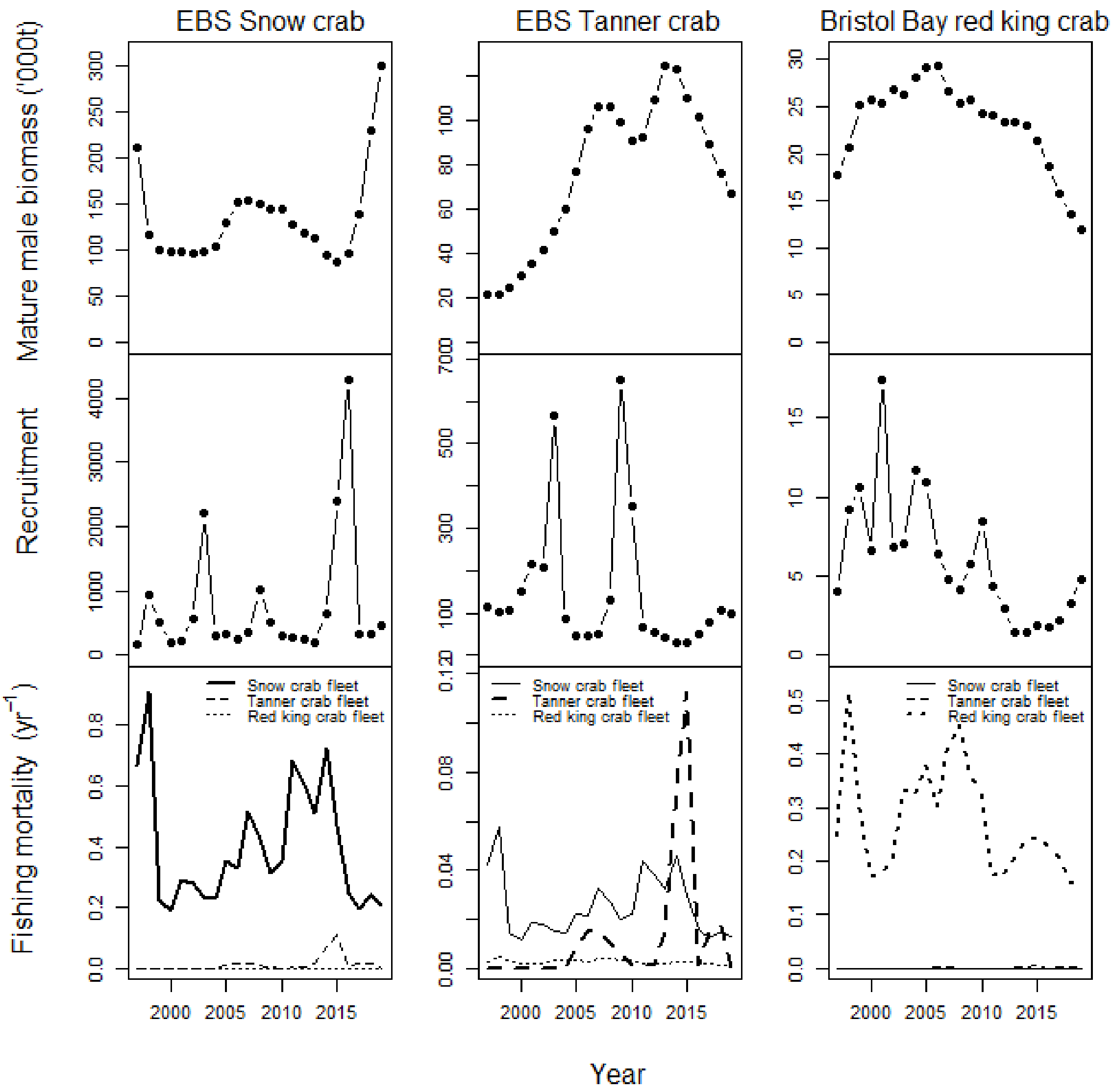

Fig. 4. Summary statistics (mature male biomass; upper panels), recruitment (center panels), and fully-selected fishing mortality (by target fleet) for the three stocks. The bolded lines in the lower panels reflect the target fleets for each stock.

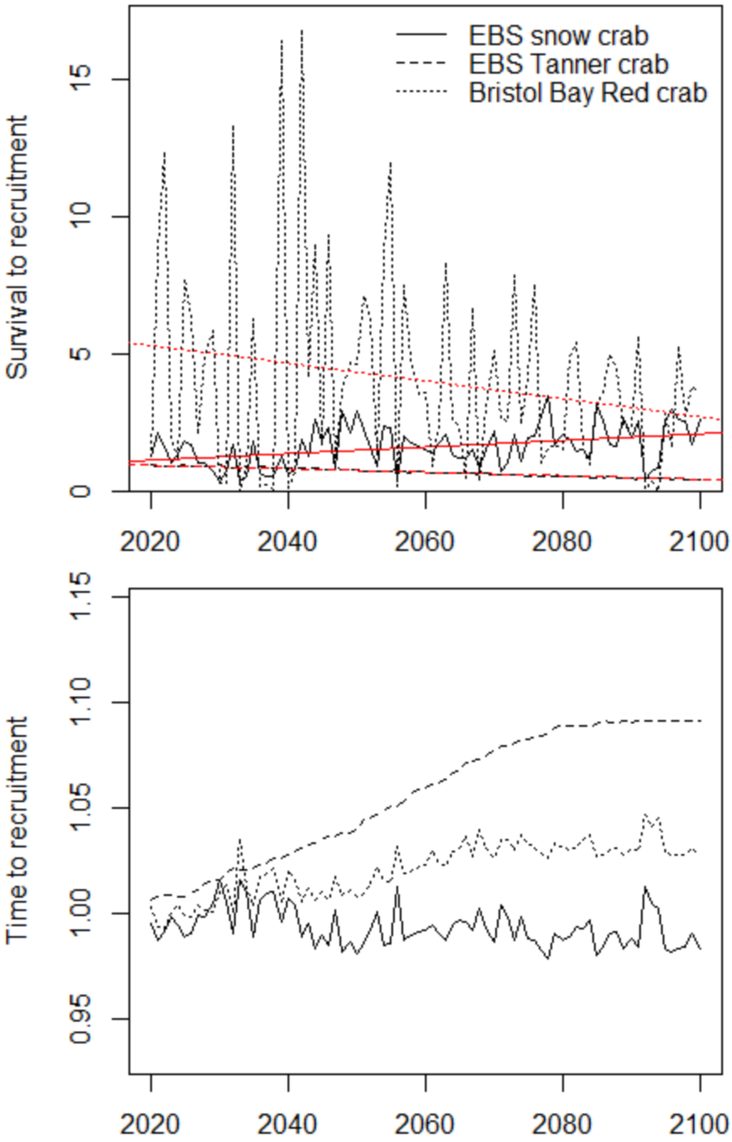

Fig. 5. Time-trajectories (2020-2100) of survival to recruitment and time to recruitment (expressed relative to the 2006-2020 averages) for EBS snow crab (solid lines), EBS southern Tanner crab (dashed lines), and Bristol Bay red king crab (doted lines) in the absence of density-dependence in survival. The red lines in the upper panel are linear fits to the survival rates for EBS snow crab, EBS southern Tanner crab and Bristol Bay red king crab. The results for EBS southern Tanner crab exhibit less inter-annual variation than those for the other species as EBS southern Tanner crab is assumed not to be impacted by temperature, which varies substantially over time.

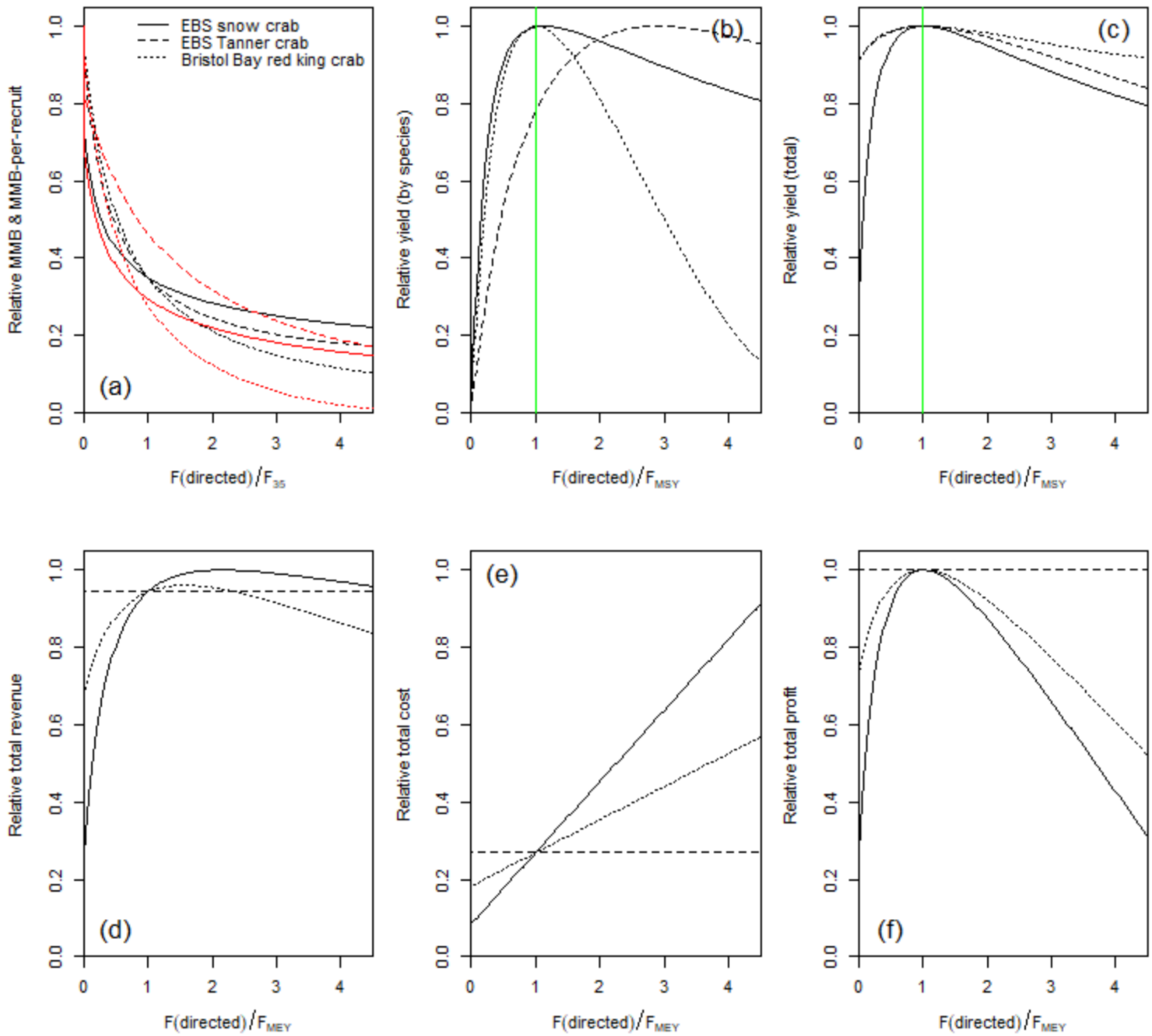

Fig. 6. Spawning biomass-per-recruit (black lines) and spawning biomass (red lines) both relative to unfished levels versus fully-selected fishing mortality (expressed relative to $F_{35\%}$) (a), yield by stock versus fully-selected fishing mortality (expressed relative to F_{MSY}) by fleet (with fully-selected fishing mortality for the remaining fleets set to F_{MSY}) (b), and relative total revenue, total cost and total profit versus fully-selected fishing mortality (expressed relative to F_{MEY}) by fleet (with fishing mortality for the remaining fleets set to F_{MEY}) (c-f). The results in this figure are based on the reference effects of temperature and ocean pH.

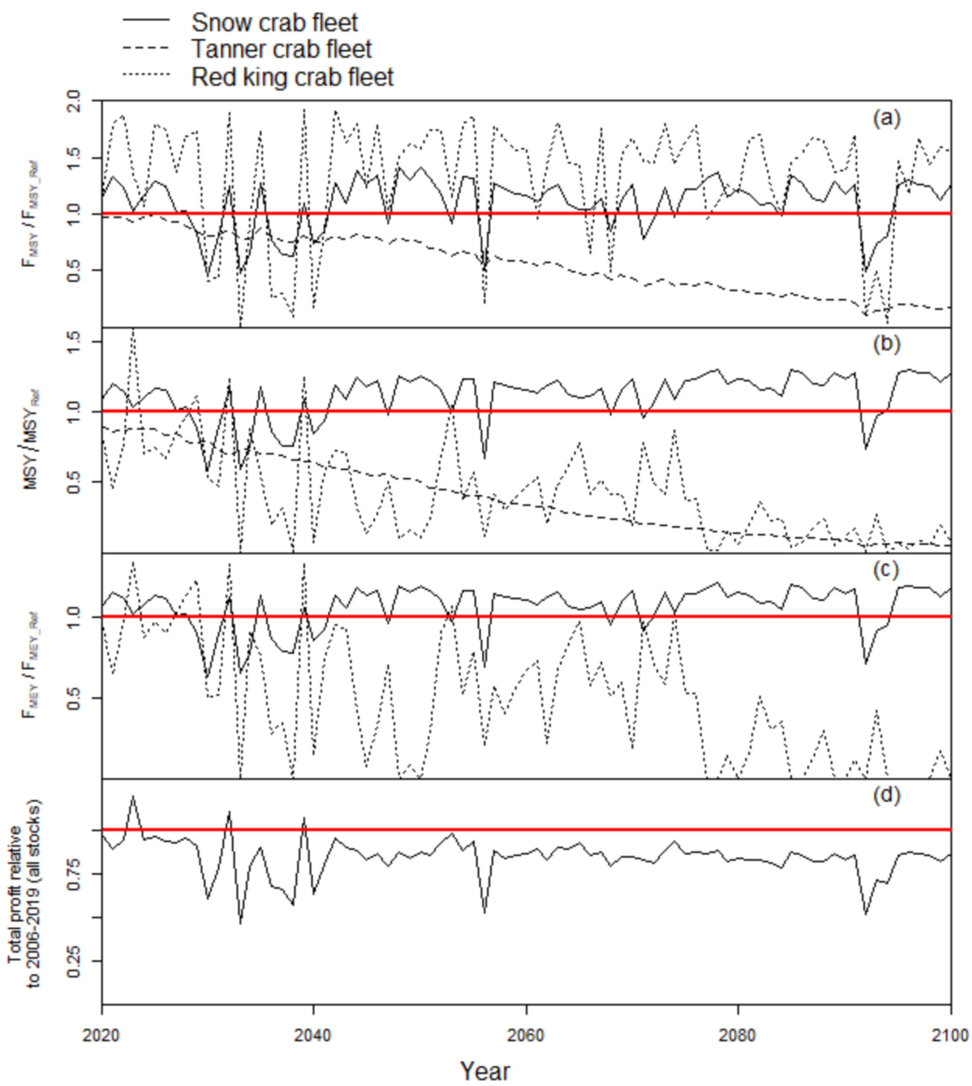

Fig. 7. Time-trajectories of the fully-selected fishing mortality at which total catch (a) and profit (c) are maximized and the catch by species (b) / total profit (d), expressed relative to the values for the reference period. The values for F_{MSY} and F_{MEY} were selected by stock for each year given the temperature and ocean pH for that year and assuming that the population is in equilibrium. Results are not visible for EBS southern Tanner crab in panel (c) as F_{MEY} for this stock is essentially zero for the entire series. There is only a single (solid) curve in panel (d) as this is a profile over all stocks.

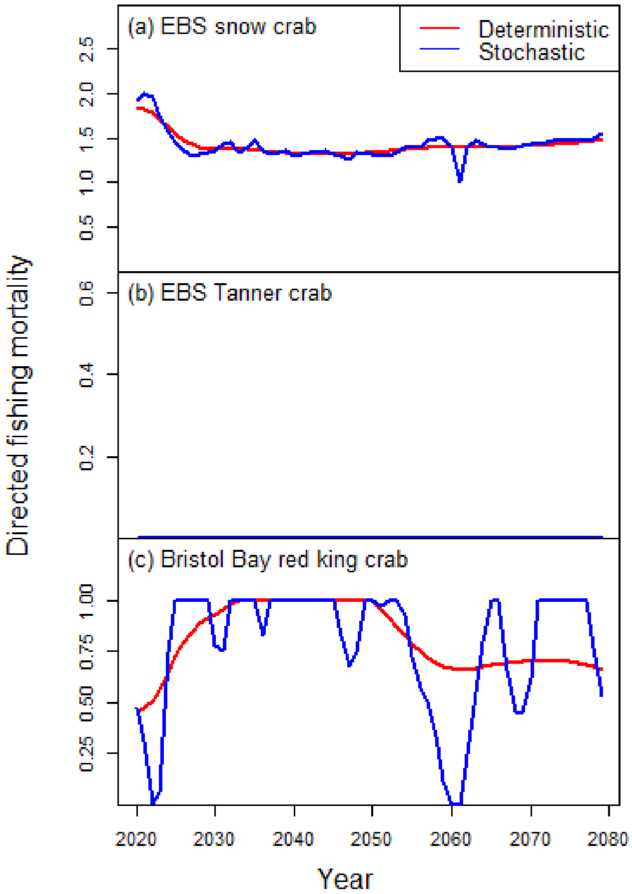

962
963 Fig. 8. Values for F_{opt}. Results are shown for $F_{opt\text{-}det}$ ('deterministic') and $F_{opt\text{-}sto}$ ('stochastic').

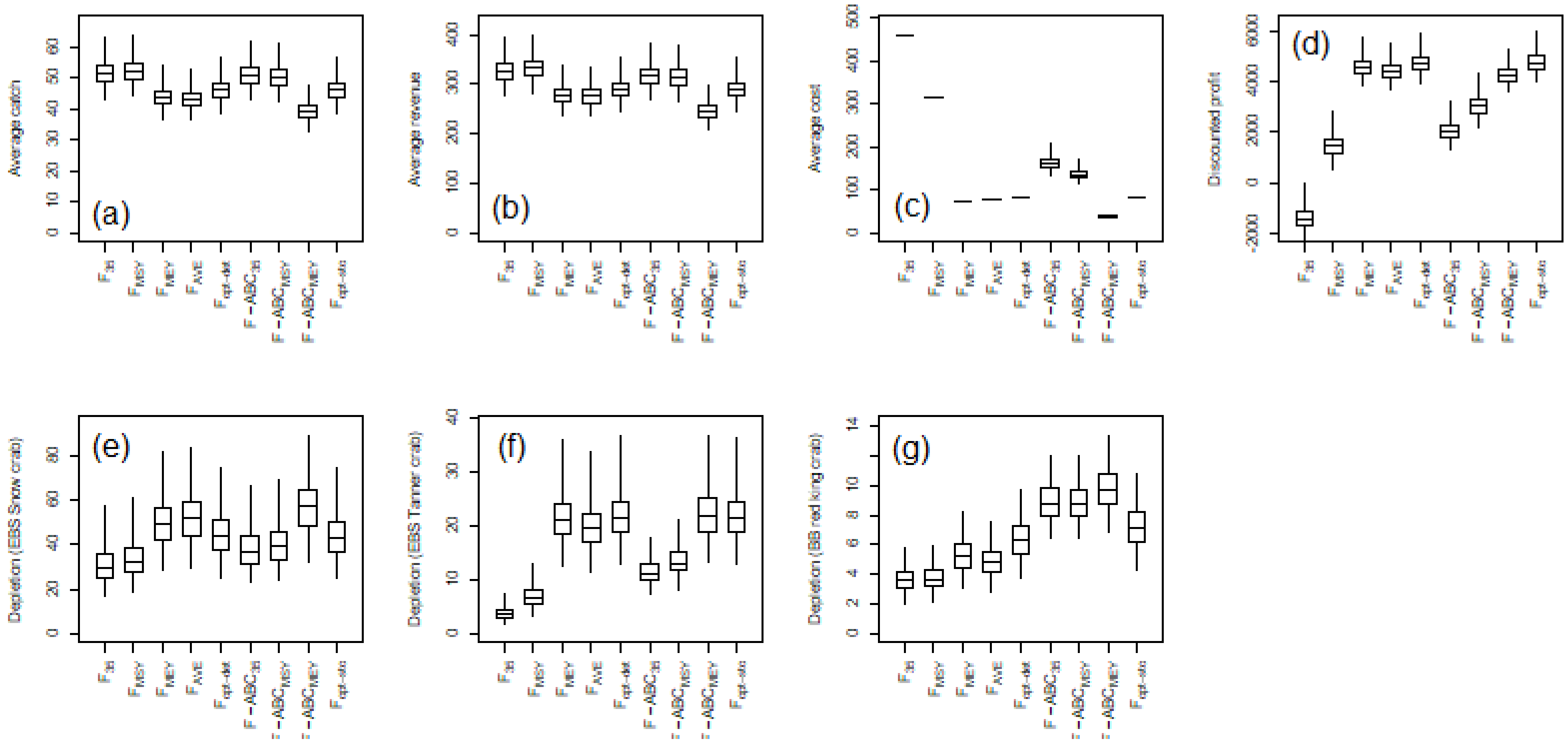

Fig. 9. Distributions (medians, and 50% and 90% intervals) for the seven summary statistics for nine harvest control rules when bycatch is not landed. The $F_{\text{opt-det}}$ and $F_{\text{opt-sto}}$ harvest control rules differ depending on whether fully-selected fishing mortality by fleet and year are selected ignoring ($F_{\text{opt-det}}$) or accounting for ($F_{\text{opt-sto}}$) variability about the stock-recruitment relationship.

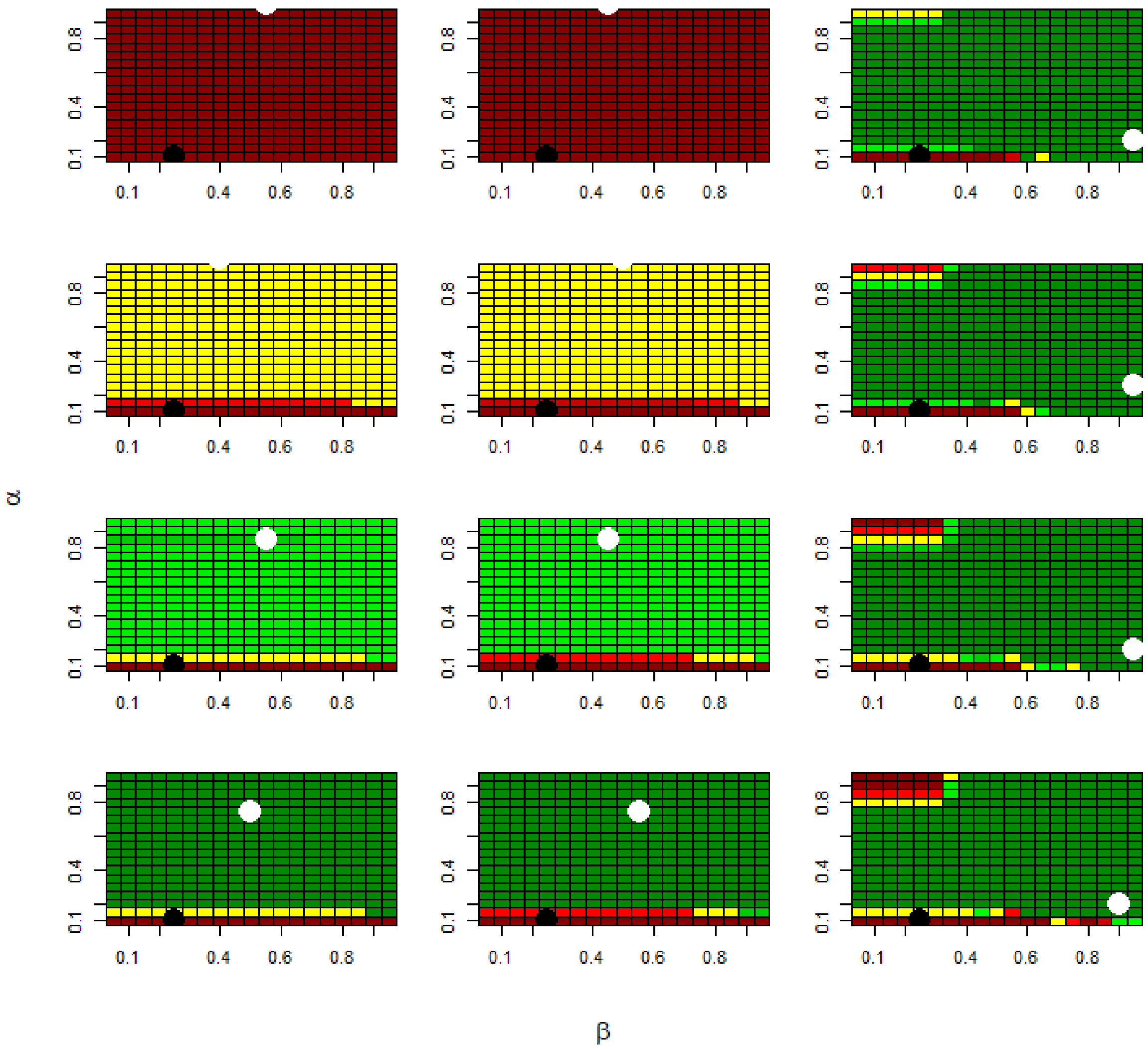

Fig. 10. Relationship between median (over simulation replicates) total discounted profit (left panels), the lower 5th percentile for total discounted profit (center panels), and the lower 5th percentile for the depletion of Bristol Bay red king crab (right panels), expressed relative to results for the F-ABC$_{MEY}$ harvest control rules given values for the parameters of the ABC harvest control rule. Values in red indicate results less desirable than for the F-ABC$_{MEY}$ harvest control rule, those in yellow within 2% of the F_{MSY}_ABC harvest control rule and those in green better than F-ABC$_{MEY}$ harvest control rule by more than 2%. The intensity of the red and green lines denotes the difference from no change. Results are shown for ABC-OFL buffers of 0.7, 0.85, 0.95 and 1.05 (rows 1-4). The black circle denotes the current choice for (α, β) while the white circle is the choice of (α, β) at which the metric concerned in maximized.